

CHAPTER 15

3D and 4D printing of biomaterials and biocomposites, bioinspired composites, and related transformers

Lewis R. Hart^a, Yinfeng He^b, Laura Ruiz-Cantu^b, Zuoxin Zhou^b, Derek Irvine^b, Ricky Wildman^b, Wayne Hayes^a

^aDepartment of Chemistry, University of Reading, Reading, United Kingdom

^bFaculty of Engineering, The University of Nottingham, Nottingham, United Kingdom

1 Introduction

Three-dimensional printing (3D printing) or additive manufacturing (AM) promises to produce complex devices formulated from biomaterials and bioinspired materials from designs that are patient-specific. Since its advent as presurgical visualization technique and fabrication of tooling molds, 3D printing has evolved to yield bespoke devices, implants, scaffolds, diagnostic devices, and drug-delivery systems. As a result of recent public interest and affordable printing platforms, there is the desire to utilize this exciting technology for personalized health care. However, before AM can become a ubiquitous tool for the regeneration of complex tissues, such as bone, cartilage, muscles, vessels, nerves, and complex organs with multifaceted three-dimensional microarchitecture (e.g., kidneys, lymphoid organs), a number of technological limitations must be overcome.

The development of advanced bioinks for 3D and 4D printing through the rational design of novel materials and their implementation as functional biomaterials through ever-expanding deposition techniques has improved the diversity and functionality of printed constructs outside of the traditional biofabrication window [1]. While there is the necessity for a compromise between suitability for purpose and biocompatibility, recent developments in materials science and bioink formulations have resulted in an improved range of solutions for biofabrication platforms. New biologically relevant printing formulations with highly consistent and accurate deposition parameters, attractive mechanical properties, high cytocompatibility, and the ability to modulate cellular functions are now being developed and offer prospects as biomaterials for use in a multitude of different applications; however, further work is needed before these novel materials become common place.

In this chapter, we explore some of the approaches being pursued to achieve these targets in common 3D and 4D printing techniques, including an overview of the state-of-the-art technologies and formulations used in novel materials and bioinks, which are currently being developed, the techniques which are being utilized to produce 3D and 4D constructs, and the applications for which these new materials may be employed in. Key examples are highlighted to demonstrate the progress of this emerging technology and limitations to its development identified.

2 Deposition techniques for 3D printing of biomaterials

This section focuses on the discussion of most commonly used AM techniques to process polymer nanocomposite biomaterials, including stereolithography (SLA), extrusion printing, inkjet printing, and selective laser sintering or selective laser melting (Fig. 1) [2]. Each of these techniques relies on different technologies to produce 3D constructs and requires different physical properties of materials in order to achieve good printability, including rheology, voxel solidification, interlayered coalescence, and dimensional accuracy.

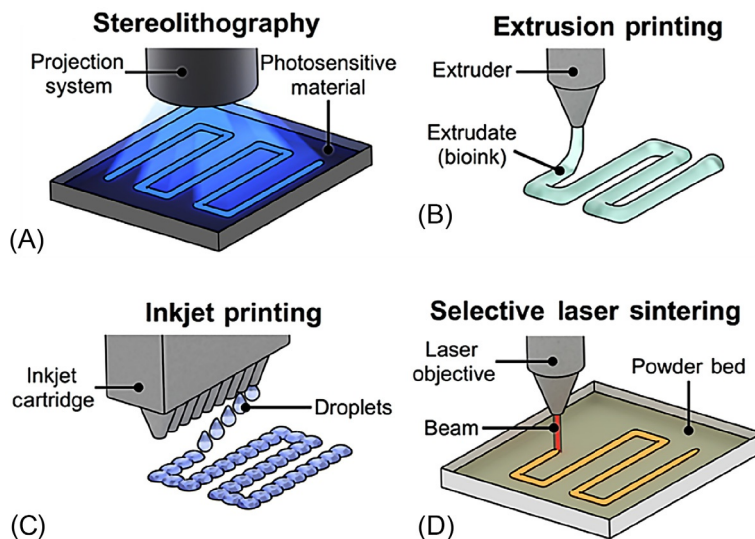


Fig. 1 Examples of common fabrication techniques adapted for biomaterials. Stereolithography (A) takes advantage of photoinduced polymerization of liquids monomers or resins in specific regions exposed to light. Extrusion printing (B) and inkjet printing (C) commonly rely on plasticized materials or solutions, which can be deposited and quickly solidify postdeposition. Selective laser sintering (D) provides localized heating to melt and fuse powder granules to produce structures. (Adapted with permission from J.S. Miller, J.A. Burdick, Editorial: special issue on 3D printing of biomaterials, *ACS Biomater. Sci. Eng.* 2 (2016) 1658–1661. Copyright (2016) American Chemical Society.)

2.1 Stereolithography

SLA uses a layer-by-layer approach to fabricate 3D microstructure. This technology encompasses traditional lithography techniques, which build geometries from top to bottom, and also digital light processing (DLP), which builds geometries from bottom to top. Both techniques rely on a UV light source and a moveable stage, which is in contact with a reservoir containing a photocurable resin to selectively cure monomers in the desired location [3]. Once a layer has been completed, a new layer of liquid resin is introduced and crosslinked with the previous layer by photoinduced polymerization. The process continues in a layer-by-layer fashion until the desired 3D object is produced [4]. In classical SLA, a liquid resin is selectively photopolymerized by a rastering laser of UV light to afford the desired structure. In newer methods such as DLP, the same basic principles are applied; however, unlike SLA, which relies on point-source illumination to pattern one voxel at a time, DLP permits a layer resin to be cured using micromirror array devices or dynamic liquid crystal masks [5] to project a mask or pattern onto the reservoir of liquid resin. As a consequence of this, DLP is generally much faster than SLA as an AM technique. Generally, SLA, and DLP in particular, are advantageous as an AM technique as the amount of resin or materials required for the manufacturing process is reduced in this material efficient technique. The main drawback of SLA is the limitation in materials available as the reagents must be UV-curable, be low in viscosity, and optically transparent to fully realize the potential of this technology.

SLA has continued to advance, resulting in the development of more precise AM techniques such as two-photon polymerization. The two-photon polymerization technique relies on focusing a laser beam into a very small volume of resin by means of a high numerical aperture objective [6]. This technique provides the highest lateral resolution (c.100 nm) by utilizing the squared point-spread function associated with the two-photon absorption of light of wavelength λ , which is confined to a tightly focused voxel (one volume element within the 3D structure) with dimensions on the order of λ^3 [7]. As is common with many 3D printing technologies, there is an inherent compromise between printer resolution, build volume, and printing speed. In this instance, highly complex microarchitectures can be constructed using two-photon polymerization, but a limit to the overall dimensions (c.1 cm³) is often observed. A significant disadvantage to these methodologies arises from their inability to pattern multiple materials in a single build sequence.

SLA has found great use for 3D printing of biomaterials, which are modified with photocurable motifs to obtain stereolithographically printable resins. Notable examples include poly(ethylene glycol diacrylate), one of the most commonly utilized biopolymer resins for SLA. This was exemplified by Palaganas et al. [8] who reported a formulation containing poly(ethylene glycol diacrylate), cellulose nanocrystals derived from the abaca plant, and a photoinitiator for use in stereolithographic AM (Fig. 2A). The biocompatible formulation was then used to produce a variety of complex architectures, including a human ear construct (Fig. 2C).

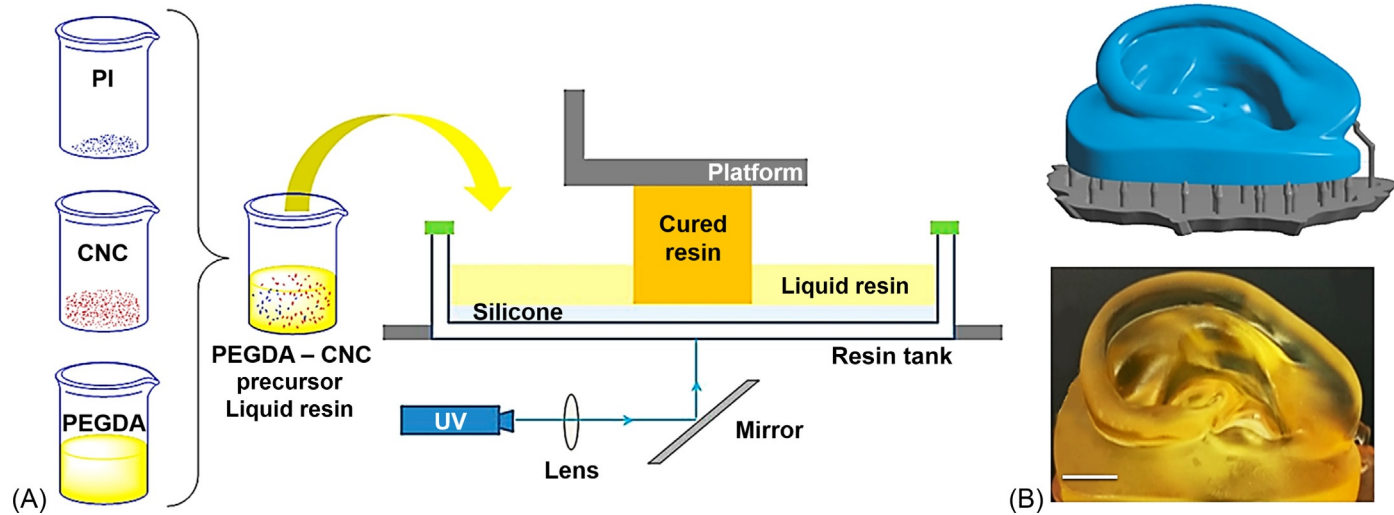


Fig. 2 (A) A photocurable resin comprising polymer matrix (PEGDA), nanoparticles (CNC), and photoinitiator (PI), which were polymerized to form a 3D geometry during the stereolithography process. (B) Design and 3D printing of human ear construct using PEGDA-CNC hydrogel via stereolithography potentially suitable for tissue engineering applications. (Adapted with permission from N.B. Palaganas, J.D. Mangadlao, A.C. De Leon, J.O. Palaganas, K.D. Pangilinan, Y.J. Lee, R.C. Advincula, 3D printing of photocurable cellulose nanocrystal composite for fabrication of complex architectures via stereolithography, *ACS Appl. Mater. Interfaces* 9 (2017) 34314–34324. Copyright (2017) American Chemical Society.)

To increase the resolution of the resulting feature, nanoparticles have been incorporated into resins, which are suitable for 3D materials fabrication by SLA. In addition, some nanoparticles also have the capability to be UV-curable; hence, they can be polymerized together with resin monomers [9]. A silk fibroin hydrogel with melanin nanoparticles has been reported [10] to improve printing resolution of a poly(ethylene glycol)-tetra acrylate bioink. A nanoparticle concentration of 1% (w/v) was sufficient to reduce resin transparency sufficiently so that the beam of light used to photopolymerize the monomers could be focused at a localized region.

2.2 Extrusion printing

AM-based melt extrusion is a common technique, which usually heats a polymer-based filament in a printhead and subsequently deposits it out of a nozzle. It is perhaps the most commonly used AM technique to process nanomaterial-incorporated thermoplastics as a result of its similarity to the traditional manufacturing routes for many polymers. The printhead temperature is set to be above the melting point of the thermoplastics, which can be up to 380°C in the case of poly(etheretherketone) (PEEK) [11]. Incorporation of nanoparticles increases the melt viscosity of the formulation and therefore a higher printhead temperature is required in order to achieve good flow of the material. Alternatively, nanoparticles can be incorporated onto the geometry after the AM process via dip coating [11,12]. Surface properties, such as biocompatibility, bioactivity, and hydrophilicity, are modified significantly as a result of coating of nanoparticle surface layers [12]. Other important processing parameters for melt extrusion-based AM include nozzle diameter, print speed, layer thickness, number of external shells, filling density, and heat-bed temperature. 3D printing process can be assisted by the design optimization based on the combination of experimental and computational analysis.

Melt extrusion can be exemplified by a study reported by Yu et al. [12] in which a 3D printed lumber cage was designed and fabricated from a polymer nanocomposite based on a polyhedral oligomeric silsesquioxane poly(carbonate-urea) urethane. The polymer was blended with hydroxyapatite nanocrystals and was 3D printed using melt extrusion into a 75% porous scaffold and then seeded with preosteoblast cells (Fig. 3A). Melt extrusion may also be combined with electrospinning to construct 3D tissue engineering (TE) scaffolds for hard tissues [13,14]. A polymer model for tendon graft healing has been reported [13] in which a bone anchor was fabricated via 3D printing of poly(lactic acid). A biomimetic patch, constructed from collagen blended with poly(D,L-lactide-co-glycolide), was then produced via electrospinning to form a nanofibrous membrane, which promoted the integration of tendon and bone during the healing process.

An alternative to melt extrusion is paste extrusion, which requires a relatively low processing temperature compared with melt extrusion, which is more compatible with the incorporated biomolecules. Paste extrusion-based AM processes different materials in

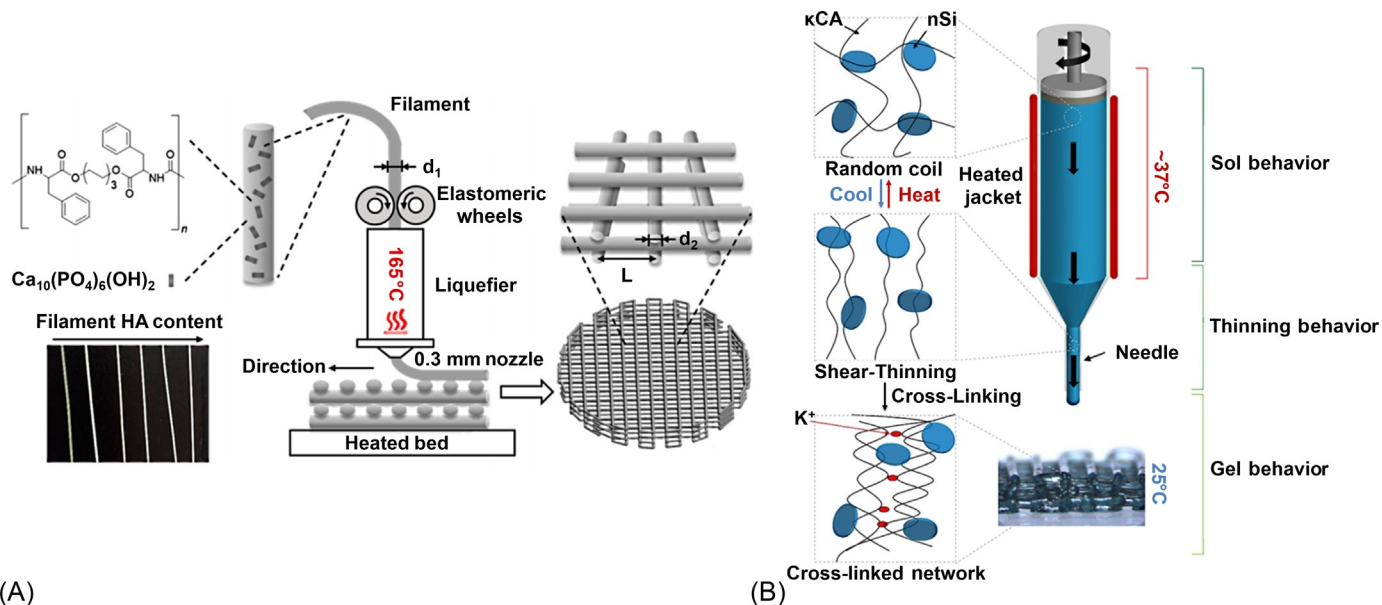


Fig. 3 (A) Melt extrusion: filament of a composite with nanohydroxyapatite (nHA) was fed into the heated nozzle and extruded to build a 3D scaffold with a series of rods layered perpendicularly. (B) Paste extrusion: thermos-reversible gelation triggered during process resulted in the formation of a stable double-helical structure. ((A) Reproduced with permission from J. Yu, Y. Xu, S. Li, G. V. Seifert, M.L. Becker, Three-dimensional printing of nano hydroxyapatite/poly(ester urea) composite scaffolds with enhanced bioactivity, *Biomacromolecules* 18 (2017) 4171–4183. Copyright (2017) American Chemical Society. (B) Reproduced with permission from S.A. Wilson, L.M. Cross, C.W. Peak, A.K. Gaharwar, Shear-thinning and thermo-reversible nanoengineered inks for 3D bioprinting, *ACS Appl. Mater. Interfaces* 9 (2017) 43449–43458. Copyright (2017) American Chemical Society.)

the form of a viscous liquid usually at a relatively low temperature when compared to melt extrusion. Materials are conveyed to a small nozzle using either piston or compressed air and subsequently deposited on the substrate. The overall structure is built according to the 3D CAD design. The challenge in this technique lies in the solidification of materials depositing out of the nozzle from a paste extrusion 3D printer. A study reported by Maurmann et al. overcame this issue as demonstrated by the use of a novel cryogenic 3D printer [15]. The geometry was built on a cryogenic print bed controlled at -30°C in order to solidify inks immediately after depositing from the nozzle. The organic solvent was subsequently removed during postprocessing using cryodrying. Alternatively, nanoparticles were added to increase the viscosity of the bioink in order to retain shapes after the ink is deposited onto the substrate. Additionally, the viscosity cannot be too high to exceed the pressure limit of the instrument.

Paste extrusion-based AM is ideal for processing hydrogels that are crosslinked by either physical or chemical interactions once the gel is deposited on the substrate. As a result of strong hydrogen-bonding interactions between *N*-acryloyl glycinamide and nanoclays, gel-like structures are afforded [16]. The printed ink can be UV crosslinked post deposition to yield a stiff material. Two-dimensional nanosilica has also been employed to tailor the shear-thinning behavior of bioinks [17]. The formulation containing κ -carrageenan, a linear sulfated polysaccharide, was blended at minimum concentration of 1.5 wt.% in order to have a viscosity that was sufficient to retain shape after being deposited. However, a gel was formed with concentrations in excess of 1.9 wt.% at 40°C as a consequence of hydrogen-bonding interactions between the constituent components. Nanosilica was also introduced to disrupt hydrogen-bonding interactions at high concentrations of κ -carrageenan and also increase shape retention after printing (Fig. 3B).

2.3 Inkjet printing

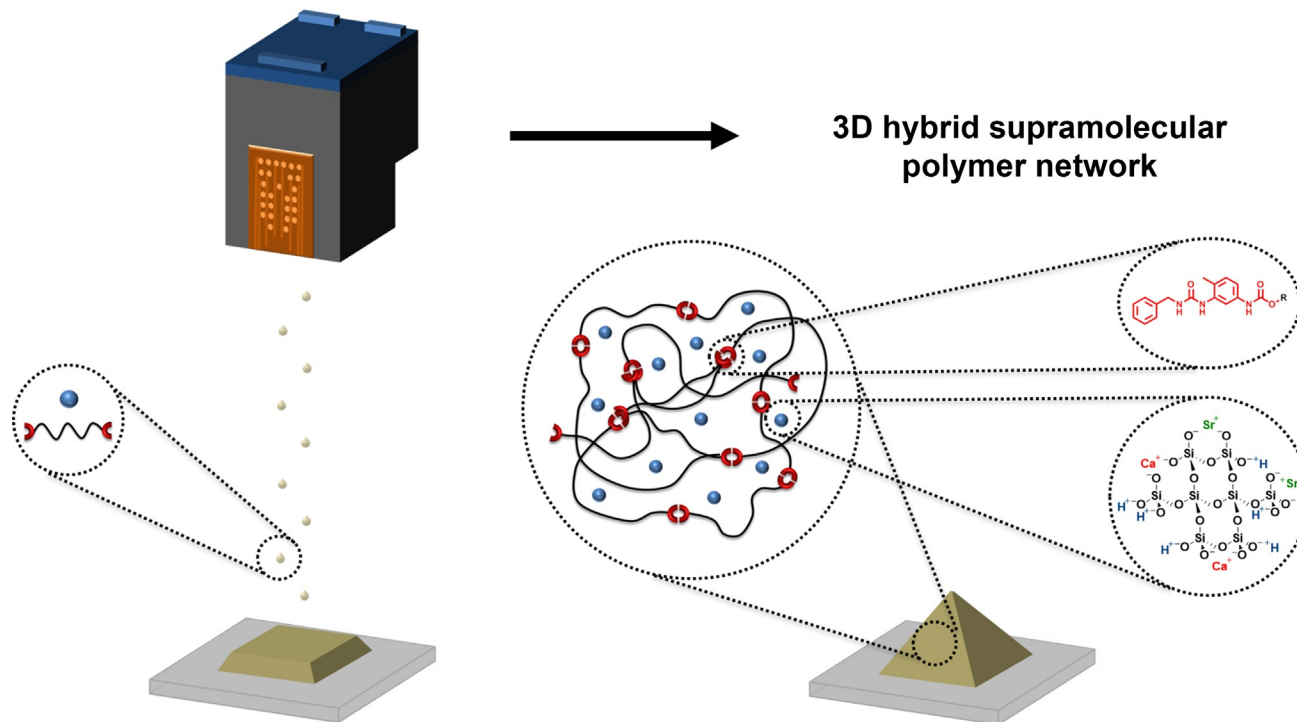
While light-based printing technologies give rise to excellent feature resolution, they are limited to fabrication with either photopolymerizable resins, which often are only able to produce rigid thermoset polymers, or thermoplastic polymer powders. By contrast, ink-based AM methods can afford ink formulations that comprise monomers, oligomers, polymers, or particulates, resulting in innumerable combinations of soft and hard matter. The choice of material may be manipulated to achieve the desired rheological behavior as dictated by the following physical properties of the inks: viscosity, surface tension, shear yield stress, and shear elastic and loss moduli; these are fundamental parameters necessary for ink-based printing, which require droplet or filament formation.

Inkjet 3D printing predominantly uses a drop-on-demand process with either a heater pad or a piezoelectric transducer to trigger ejection of low-viscosity ink droplets from an

array of nozzles, analogous to 2D printing technologies. A number of inkjet printing techniques use this approach to form 3D structures, including direct inkjet printing, hot-melt printing, and inkjet printing onto powder beds. In all instances, the density (ρ), viscosity (μ), surface tension (γ) characteristic droplet diameter of the ink formulation, as well as the velocity of the ejected droplet (v) and the nozzle diameter (d) are vital parameters which must be carefully controlled to successfully produce the desired features. As a result of the summation of these parameters, it is challenging to stably jet complex fluids containing high polymer concentrations or indeed composite materials with particulates exceeding 100 nm in diameter, or at concentrations in excess of a few percent. However, the drawbacks of inkjet printing are outweighed in many instances by tremendous advantages of this technique, arising from highly sophisticated printhead designs. State-of-the-art, multinozzle arrangements, which can deposit multiple materials simultaneously with great accuracy, enable highly complex constructs to be afforded. Inkjet printer design is also crucial in producing high-quality biomaterial constructs. A piezoelectric print head, in which the movement of a piezoelectric actuator creates a pressure variation within the ink at the nozzle and thus subsequently ejecting ink droplets from the nozzle, is favorable as it allows a wider range of ink formulations to be processed without loss of performance or unwanted corrosion within the printer cartridge. Additional solvent can also be used to reduce the viscosity of ink formulation to be within the printable range, which is critical for inkjet printing [18,19]. Solvent is removed after the process leaving the functional materials on the substrate.

Inkjet printing has predominantly been used for building microscale patterns or coatings as a result of its high resolution. For example, functional silver nanoparticle formulated with chitosan has been printed to overcoat a thermoset polymer surface, used for cranial reconstruction. Full coverage was achieved by adjusting the droplet spacing during the process [20].

Nanocomposites are often suspended in a solvent to prepare ink formations for inkjet printing. Antibiotic micropatterns have developed to prevent the formation of biofilm colonies and also promoted osteogenic cell development on orthopedic implants [18]. The ink formation contained rifampicin, poly(D,L-lactide-co-glycolide), calcium phosphate nanoparticles suspended in solution. Crucially, the concentration of nanoparticle must be controlled to avoid forming agglomeration and clogging the nozzles. A recent study (Scheme 1) has developed silica nanoparticles-incorporated supra-molecular biopolymers, which were mixed with a solvent of high boiling temperature and low vapor pressure [19]. The low-molecular-weight polymer was capable of self-assembly into a pseudo-high-molecular-weight polymer network upon deposition to form 3D constructs. The resulting 3D printed structure was shown to be biocompatible and as such the biomedical scaffolds have potential applications such as regenerative medicine.



Scheme 1 Supramolecular polymers incorporated with silica nanoparticles were deposited simultaneously using inkjet printing to form a 3D network. (Reproduced with permission from L.R. Hart, S. Li, C. Sturgess, R. Wildman, J.R. Jones, W. Hayes, *3D printing of biocompatible supramolecular polymers and their composites*, ACS Appl. Mater. Interfaces. 8 (2016) 3115–3122. Copyright (2017) American Chemical Society.)

2.4 Selective laser sintering/melting

Selective laser sintering is an AM technique, which binds together thin layers of powder particles using a CO₂ or Nd:YAG laser beam to produce 3D objects [21]. By slicing the digital, computer-aided design (CAD) image, each layer of the pattern can be assembled sequentially to build a 3D construct in a layer-by-layer approach. During the fabrication process, the laser scans across the surface of the powder bed, containing either polymeric or metallic particles, in a specific 2D pattern to sinter or fuse them by heating them in excess of the glass transition or melt temperature. Molecular diffusion along the outermost surface of the individual particles leads to neck formation between neighboring particles. After a layer is completed, a new bed of powdered polymer or metal is placed over the top surface of the sintered material to enable the next layer of structure to be formed. Three distinct categories of sintering technology can be classified: Solid-state sintering, Liquid-phase-assisted sintering, and full melting [21]. While solid-state sintering can be achieved in most instances between T_m and $T_m/2$, the technique of full melting, as the name suggests, requires the powder to be heated above the materials melting point using an intense energy beam to completely fuse the particles into one fully dense, consolidated structure. Liquid-phase-assisted sintering involves the addition of a lower melting point additive to the matrix phase and is commonly used for materials that are difficult to sinter such as ceramics. Commonly, a small amount of polymeric material is added to the ceramic, which facilitates the fabrication of 3D constructs.

The material properties and process factors such as laser energy density, the laser scan speed, particle size, particle bed temperature, layer thickness, and hatch distance can affect the structural and mechanical properties of fabricated parts. Selective laser sintering or melting has the advantage of producing structures with almost full relative density, which has been a major issue for many other AM techniques. The relative density reported for selective laser melting of 316L stainless steel has reached in excess of 99.9% [22,23], while selective laser melting of the titanium alloy Ti6Al4V and cobalt-chromium has also achieved high relative densities of 99.8% [24] and 99.94% [25], respectively. As a result, excellent mechanical properties have been obtained using selective laser sintering, which are comparable to the same structures fabricated using traditional manufacturing routes. The fast cooling of the selective laser sintering process often results in a refined microstructure of the material fabricated. For example, a fine cellular dendritic microstructure has been observed from SLM 316L stainless steel. The tensile strength was thus increased, but the ductility had been reduced compared to stainless steel parts made using forging [26–30]. It has been shown that cell attachment is affected by the surface roughness of the 3D printed construct. Selective laser-sintered parts usually have surface roughness of approximately 20 μm , which can be improved during post-processing. However, surface roughnesses of 5.82 μm [31] and 2 μm [23], respectively, have been reported from selective laser-sintered parts from 316L stainless steel. Structures with a gradient porosity have also been made to balance the mechanical strength and tissue ingrowth in the porous area (Fig. 4) [32].

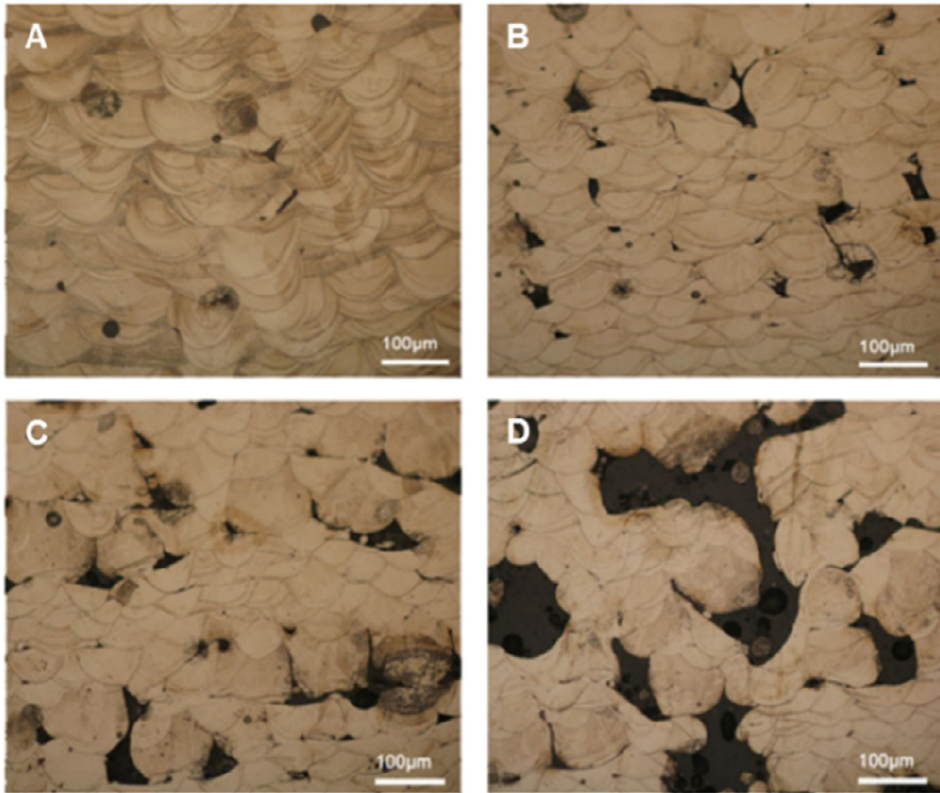


Fig. 4 Metallographs showing the porosities variation in 316L stainless steel by gradient speeds direction (A = 90 mm s^{-1} , B = 120 mm s^{-1} , C = 150 mm s^{-1} , D = 180 mm s^{-1}). (Reproduced with permission from J. Delgado, J. Ciurana, C.A. Rodríguez, *Influence of process parameters on part quality and mechanical properties for DMLS and SLM with iron-based materials*, *Int. J. Adv. Manuf. Technol.* 60 (2012) 601–610. Copyright (2009) Springer Nature.)

3 Materials for 3D printing of biomaterials

The advancement of 3D printing in the past decade in fields such as TE, medicine, and dentistry has led to an increase in the pallet of materials, which are available to engineers, chemists, and biomedical scientist to construct functional devices and objects [33]. The spectrum of materials available extends from hard matter such as metals and ceramics to soft matter such as polymeric materials and biological tissues [34]. This diversity is further extended with composite materials, which are able to take advantage of the inherent characteristics of the constituent materials and blend these in such a way as to exploit their properties in a new manner. Although the library of materials available to engineers, chemists, and biologist is expanding, novel materials are required to further develop this

exciting area of research. This section intends to provide the reader with an overview of the pallet of materials available for manufacturing constructs from biomaterials, giving key examples from the literature. The reader is directed to number of excellent reviews in the areas of hard matter [2, 35], soft matter [36, 37], biological materials [38–40], and composites [41], which describe each individual class of material in depth.

3.1 Hard matter

In recent years, the number of AM processes using metallic materials has experienced rapid growth. This increase has not only been observed in fundamental research, but also in commercial applications [42]. 3D printing of metals provides both freedom of design and high precision while retaining good materials efficiency and modest build speeds; however, it can be an extremely costly process [43].

Steel is perhaps the most commonly engineered material worldwide and is therefore of great interest to the AM community. Different grades of steel are available for 3D printing, each tailored to specific applications based on material characteristic [35,44–47]; however, it is austenitic grade 316L stainless steel, which has found predominant use in biomaterial applications. In 2009, Li et al. offered an early insight into AM of steel components for biomedical applications by fabricating a 316L stainless steel object with a pore gradient structure by selective laser melting [32]. By careful control of the scan rate, the morphology of the object could be controlled as demonstrated by metallography and tensile experiments. Well-defined and structurally robust regions were produced to provide strength to the object, while domains of porosity could be achieved by increasing the scan speed, which could be utilized to promote tissue cell growth. Dong et al. have built upon these results and reported [48] the selective laser sintering of a fine powder of 316L grade stainless steel as biocompatible and corrosion-resistant materials for medical implants. By controlling the power of the laser, morphological control of the grains afforded could be achieved, in addition to mechanical properties such as ultimate tensile strength (600–620 MPa) and yield strength. Biocompatibility studies were also conducted, which revealed good cell viability and proliferation over an extended time period. 3D Printed 316L grade stainless steel has also been deployed in dental applications. Bibb et al. have reported [49] a biocompatible removable partial denture as a metallic framework. The custom-fit denture framework was built using support structures, which were removed by hand before finishing and polishing was complete. While the framework demonstrated a good fit, the dental clasps were permanently deformed after multiple insertions and removals of the denture, reducing the ability of the framework to grip and thus resulting in the teeth and the denture becoming loose.

A number of other metals, such as titanium and its alloys, magnesium alloys as well as cobalt–chromium alloys, have been used in AM process to produce a variety of implants. For example, Murr et al. have demonstrated [50] the fabrication of biocompatible and

patient-specific total knee implants using electron beam melting of Co-29Cr-6Mo and Ti-6Al-4V to give varying density open cellular structures. The Ti-6Al-4V solid created by electron beam melting exhibits an α -phase, acicular platelet microstructures similar to commercial, wrought products, while the mesh and foam prototypes exhibit α' -martensitic platelets or mixtures of α and α' platelets, which are spatially smaller than the solid α -phase platelets, giving rise to harder structures and correspondingly higher strength materials. Interestingly, solid, mesh, and foam Co-29Cr-6Mo prototypes all exhibited a directional, columnar Cr₂₃C₆ precipitate architecture parallel to the build direction intermixed with some stacking faults in the fcc matrix. After annealing, these precipitates dissolved and were replaced by a higher density of intrinsic stacking faults, which kept the hardness essentially constant. A porous biomaterial comprising TiO₂ nanotubes loaded with silver antimicrobial agents has been reported by Yavari et al. [51] Nanotubes were prepared using an optimized anodizing protocol on the surface of porous titanium scaffolds, which had been deposited by direct metal printing. The nanotubes were then loaded by submerging in AgNO₃ solutions at different concentrations. By assessing the antimicrobial behavior and cell viability of the biomaterial, the nanotubes were found to be effective in preventing biofilm formation and decreasing the number of planktonic bacteria for up to two weeks.

AM has become a vital tool for manufacturing biomaterials and tissue constructs from advanced ceramics. Habibovic et al. [52] have demonstrated the use of brushite and monetite minerals to create cementitious implants with controlled geometries, building on previous studies by Barralet and coworkers [53]. After hardening, post deposition, the compressive strength of the brushite and monetite cements was 21.7 MPa and 8.3 MPa, and the diametric tensile strength was 7.4 and 1.4 MPa, respectively. The stable materials then underwent in vivo testing for 12 weeks in goats, which revealed the materials to be biocompatible and allowed for new bone growth to be observed. Intramuscular implantation of both brushite and monetite ceramics demonstrated their osteoinductive potential. Tarafder et al. [54] have reported a biodegradable β -tricalcium phosphate-derived material, which is able to mimic bone, doped with differing ratios of SrO and MgO. By doping the β -tricalcium phosphate scaffolds, a 37%–41% improvement of the mechanical performance was observed when compared to the undoped β -tricalcium phosphate alone. The in vivo biological performance of the doped material was also observed to improve by way of a significantly higher osteoid, bone and haversian canal formation, within the materials.

3.2 Soft matter

Polymers are perhaps the most abundant feedstock for the 3D printing industry as a result of their diversity, highly customizable chemistries, precise deposition geometries, and cost effectiveness [3]. Polymers for AM are often in the form of thermoplastics, reactive

monomers, resin, or powders. In 2012, the *in vivo* biodegradation and biocompatibility of a 3D printed hydroxyl-functionalized poly(caprolactone) [47.1 kDa ($\bar{D} = 1.9$)], which exhibited enhanced hydrophilicity, increased degradation rate, and improved cell attachment, was reported by Hennink and coworkers [55]. After subcutaneous implantation in mice, 60% of the functionalized polymer mass was lost in 3 months through loss of the hydroxymethylglycolide moieties. The extent of tissue-scaffold interactions as well as vascularization was shown to be higher for the functionalized polymer compared to pure poly(caprolactone) alone. Blending of poly(lactic acid) into poly(caprolactone) matrices (50/50 wt.%) has been described by Patrício et al. [56] for use in TE. The two polymers were combined by either melting, blending, or solvent casting to afford materials suitable for extrusion printing. The biocompatible constructs produced from solvent casting to produce the polymer blend revealed improved cell adhesion and physical strength while producing uniformly interconnected pores when compared to the material afforded by melt blending. The incorporation of poly(lactic acid) to the poly(caprolactone) network also enhanced the biomechanical performance of the polymer construct when compared to poly(caprolactone) alone. Oligomers have also found use in 3D printing, for example Sturges et al. [57] have demonstrated the first use of reactive jetting to construct 3D structures comprising a two-part poly(dimethylsiloxane) ink solution, jetted as 60 wt% solutions in octyl acetate with a viscosity of less than 30 mPa s. The oligomers were printed individually onto treated substrate surfaces before curing to fabricate a complex and highly crosslinked 3D geometry without the need for support structures. Feature resolutions up to 48 ± 2 mm (X, Y) were afforded from the biocompatible polymer, and curing analysis revealed a homogeneous material was afforded. By increasing the temperature of the substrate surface, the rate of curing was increased with no discernible difference in material composition.

Lithography-based AM technologies have become appealing methods to fabricate biomaterials for use in a variety of biomedical applications. Monomers have also been utilized in formulation to form biomaterials. An early example reported by Cooke et al. [58] in 2002 featured a biodegradable resin mixture of diethyl fumarate monomer and poly(propylene fumarate) macromonomer, which was used to form biodegradable scaffolds for bone ingrowth by SLA techniques. When photocrosslinked, the resulting porous polymer exhibited an elastic modulus of 20–200 MPa and fracture strength of 20–70 MPa depending on the stoichiometry of the diethyl fumarate monomer present in the final polymer network. The mechanical properties were comparable to trabecular bone and thus make the afforded polymer an appropriate material for the manufacture of porous scaffold geometries suitable for tissue-engineered prosthetic implants. Novel monomers based on vinyl esters have been prepared by Heller et al. [59] for use as biomedical scaffolds. *In vitro* cytotoxicity studies with osteoblast-like cells demonstrated that a fatty acid trivinyl ester and divinyl ester crosslinkers were noncytotoxic, while photo-DSC was used to probe the photoreactivity of the monomers. Furthermore,

osteoblast-like cells were successfully seeded onto model polymers UV-cured on a glass substrate. The best-performing copolymer possessed a Young's modulus of 1.7 GPa and a flexural strength of 58 MPa. To complete the study, a 3D printed structure was then fabricated by SLA and the vinyl esters scaffold implanted into surgical defects in the distal femoral bone of adult New Zealand white rabbits. The obtained histological results confirmed the biocompatibility of vinyl esters and revealed the interaction between the novel biomaterial and living tissue.

Polymers have also been used to form hydrogels, for example West and coworkers have reported [60] photoactive poly(ethylene glycol) as a model material for creating substrates. Using masks, monoacrylate-terminated poly(ethylene glycol) appended to peptides were subsequently reacted to form hydrogels with defined patterns in 2D, while unreacted macromonomers were washed away with a PBS solution. The concentration of bound peptide was controlled easily by varying the concentration of the peptide-containing macromonomer as well as irradiation time. Furthermore, multiple peptides could be affixed to the hydrogel by changing the feed stock in a controlled manner. 3D hydrogel structures were then realized by the addition of a diacrylate functionalized polymer, which was formulated with the photoactive peptide macromonomer and subsequently crosslinked using UV light. The hydrogels were then assessed for their feasibility for guiding cell behavior and human dermal fibroblast adhesion onto their surfaces.

3.3 Biologically derived materials

Many of the examples of 3D printing of biologically derived materials require the use of multiple different components to build structures, which have the correct physical and biological properties to allow cells to proliferate while having the mechanical integrity needed to support the newly forming tissue. For this reason, 3D printing is an ideal tool to develop multimaterial constructs to mimic features found in the natural world; this is often achieved by means of hydrogels.

Proteins, peptides, and amino acid are also useful scaffold materials for use in 3D printing of biomaterials. Modified gelatine is often found in 3D printed biomaterials. Dubruel and coworkers [61] have reported the fabrication of high viability 3D printed macroporous materials constructed from a gelatine methacrylamide derivative. Scaffolds were designed with an interconnected pore network in the gelatine concentration range of 10–20 w/v % and control over the deposited strand dimensions was observed as a result of the physical properties of gelatine methacrylamide hydrogels. Consequently, constructs were shown to possess appropriate stiffness and high shape reliability. Furthermore, hepatocarcinoma cell line-laden gelatin hydrogels were produced without the need for viscosity-enhancing additives. The induced shear stress, curing irradiation dose, and the applied photoinitiator did not hinder cell viability (>97%). Biomimetic architectures have also been reported [62] by Gauvin et al. in which methacrylate functionalized

gelatine has been synthesized to form hydrogels. The hydrogels were then crosslinked in the presence of UV light with both single-layer (2D) and multilayer (3D) structures with precise internal architectures afforded. Human umbilical vein endothelial cells were then seeded into the structure by incubation of the cell suspension. The interconnectivity of the pores within the structure gave rise to uniform cell distribution throughout the scaffolds, resulting in high cell density and homogeneous distribution. Variation of the porous architecture (hexagonal or log pile) and methacrylate functionalized gelatine concentration resulted in control of the mechanical properties of the scaffolds. Wallace and coworkers have produced discrete layers of primary neural cells encapsulated in a peptide-modified biopolymer (gellan gum-RGD) hydrogel combined with primary cortical neurons to demonstrate a new method to 3D bioprint brain-like structures [63]. The modified gellan gum hydrogel was found to have a dramatic positive effect on primary cell proliferation and network formation as demonstrated by successful encapsulation, survival, and networking of primary cortical neurons and glial cells. The constructs afforded demonstrate usefulness in applications ranging from cell behavior studies, understanding brain injuries and neurodegenerative diseases to drug testing. Cannon and coworkers have recently reported [64] a collagen-based bioink as a human corneal stroma substitute. This proof-of-concept study formulated low-viscosity formulations containing Sodium alginate and methacrylate-containing type I collagen in different ratios to create scaffolds with structural integrity. Human corneal keratocytes were then encapsulated and the resulting material exhibited high cell viability after 1 day postprinting (>90%) and 1 week postprinting (83%).

Synthetic and biological materials can be used in conjunction to form dual networks with biological activity. Lee et al. have confirmed [65] the feasibility of fabricating an ear-shaped scaffold from poly(caprolactone) and a cell-laden alginate hydrogel for use in regenerative medicine. The construct also included sacrificial poly(ethylene glycol) layers, which were removed post deposition to form a complex porous structure, similar to those found in the human body. Cartilage and fat tissue were induced to regenerate efficiently via chondrogenesis and adipogenesis as a result of chondrocytes and adipocytes, derived from adipose-derived stromal cells, which were encapsulated within the hydrogel.

3.4 Composite materials

By combining material classes and printing these simultaneously, the structural complexity and functional performance of 3D printed constructs can be greatly enhanced. To achieve this, however, printing technologies require excellent degrees of spatial and compositional precision. Composites have also been reported for use in biologically relevant applications. Natural composite materials, such as bone and wood, are typically bonded by the combination of platelets or fibers, which reinforce the materials into yield complex

architectures. These features result in properties that exceed the sum of their parts, often combining stiffness, low density, and high strength.

Hard matter composites such as hydroxyapatite/apatite-wollastonite glass-ceramic composites have been fabricated [66] in situ by Suwanprateeb et al. with mean green strength of 1.27 MPa, which was sufficient to enable handling. Sintering at 1300°C for 3 hours gave the best-performing material (flexural modulus = 34.10 GPa, flexural strength = 76.82 MPa), which was correlated with a decrease in the porosity of the composite as a result of liquid-phase sintering. Bioactivity testing in simulated body fluid and in vitro toxicity studies revealed that the ceramic composite was nontoxic in addition to being bioactive, with osteoblast cells were observed to attach and attain normal morphology on the surface of the composite. Bergmann et al. have reported [67] bone substitute material comprising biodegradable β -tricalcium phosphate. By combining this material with a bioglass comprising SiO₂ (45.35%), Al₂O₃ (0.14%), TiO₂ (0.02%), CaO (24.92%), Na₂O (23.10%), and P₂O₅ (6.21%), a granular formulation was produced for layer-by-layer AM. The powder (layer thickness = 50–75 μ m) was then bound using an inkjet-printed solution of orthophosphoric acid and pyrophosphoric acid, which is able to react with the β -tricalcium phosphate to form a bone cement comprising dicalcium hydrogen phosphate and dicalcium pyrophosphate. The bioresorbable material was post deposition hardened by annealing at 1000°C to yield materials with a bending strength of 14.9 ± 3.6 MPa.

Synthetic polymers are amenable to formation with fillers to enhance their physical and biological characteristics. In 2015, Wei et al. [68] demonstrated the first example of a biocompatible graphene composite material comprising up to 5.6 wt% graphene dispersed in poly(acrylonitrile-butadiene-styrene). Raman spectroscopy, UV-Vis spectroscopy, and SEM were used to confirm the presence and exfoliation of the graphene sheets within the polymer matrix, thus determining good dispersion of the filler material. The maximum electrical conductivity of the cast polymer composite was measured as 6.4×10^{-5} S m⁻¹ with 3.8 wt% graphene; when 3D printed, this reduced to 2.5×10^{-7} S m⁻¹ as a result of internal voids formed during the printing process, although still presents the potential for conductive polymers to be printed. Fillers, which are able to provide mechanical strength and mimic bioglasses, have also been reported by Hayes and coworkers [19]. A novel supramolecular polymer composite has been 3D inkjet printed to generate constructs in a proof-of-concept study. The biodegradable poly(caprolactone), decorated with self-assembling recognition motifs, was formulated with silica nanoparticles to form dual organic/inorganic networks. The biocompatible hybrid scaffolds were deposited to form self-supporting structures, which revealed cell attachment to demonstrate their potential use in regenerative medicine. A hybrid inkjet printing/electrospinning system for TE applications has been disclosed [69] by Xu et al. to fabricate viable cartilage tissues. Poly(caprolactone) fibers were created and deposited by an electrospinning printhead before rabbit elastic chondrocytes, suspended in a

fibrin-collagen hydrogel, were printed concurrently in order to fabricate a five-layer tissue construct of 1 mm in thickness. The chondrocytes printed within the hybrid construct were more than 80% viability one week after printing and the cells proliferated and maintained their basic biological properties within this time. Moreover, the hybrid scaffold demonstrated enhanced mechanical properties ($E = 1.76$ MPa) compared to conventional hydrogel constructs ($E = 0.41$ MPa) generated using inkjet printing alone and electrospun poly(ϵ -caprolactone) ($E = 0.77$ MPa). Kotz et al. have reported [70] a nanocomposite comprising transparent fused silica glass embedded in a polymer matrix. Silica particles (c.40 nm in diameter) were dispersed in a monomeric matrix of hydroxyethylmethacrylate to afford constructs, upon irradiation with UV light and heat treatment, with a resolution of a few tens of micrometers. The printed fused silica glass was nonporous, with the optical transparency of commercial fused silica glass, while retaining a smooth surface. Indeed, by doping with metal salts, colored glasses can be created for use as optical filters and enabling the creation of arbitrary macro- and micro-structures in fused silica glass. In 2014, Lewis and coworkers reported [71] an artificial network of blood vessels from a gelatine methacrylate-derived UV-curable formulation containing fibroblast cells to form a biocompatible extracellular matrix (ECM). A poly(ethylene oxide)/poly(propylene oxide) copolymer, which is able to undergo thermally reversible gelation (about 4°C), was 3D printed to form 1D, 2D, or 3D vascular networks, which were encapsulated in the ECM formulation and chilled below 4°C to liquefy and remove the polymer to yield open channels, which may find use as artificial organs. Human bone morphogenetic protein-2 (rhBMP-2)-loaded poly(lactic acid) scaffolds filled with calcium phosphate (CaP) nanoparticle have been described [15] by Maurmann et al. to produce porous scaffolds. The 3D geometry was constructed by alternating layers of rhBMP-2 loaded poly(lactic acid) and layers of CaP-filled poly(lactic acid) in order to obtain a hierarchical porous scaffold structure. Multicomponent composites have also been reported such as a poly(ϵ -caprolactone)/hydroxyapatite/carbon nanotube mixture reported by Gonçalves et al. [72] The resulting slurry possessed a viscosity between 2.5 Pa s and 7 Pa s by solvent evaporation and was deposited using a paste extrusion 3D printer with a 0.45-mm-diameter needle.

Biologically derived polymer composites such as an alginate bioink that incorporates nanofibrillated cellulose has been reported by Gatenholm and coworkers [73]. The formulation takes advantage of the shear thinning and mechanical properties of the nanofibrillated cellulose combined with the rapid crosslinking capability of alginate to enable the bioprinting of living soft tissue with human nasoseptal chondrocyte cells. Anatomically shaped cartilage structures, such as a human ear, were 3D printed using magnetic resonance imaging (MRI) and computed tomography (CT) images as models. Human chondrocytes were also bioprinted in the noncytotoxic, nanocellulose-based bioink, which exhibited a cell viability of 73% and 86% after 1 and 7 days of 3D culture, respectively. 3D printed with nanoporous hydroxyapatite granulates to form scaffolds with

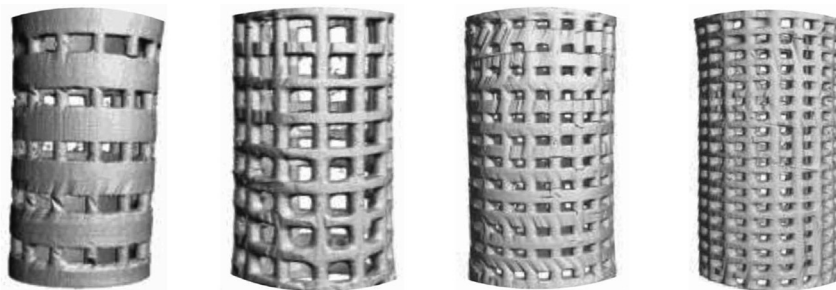
interconnected and tailored pores, ranging from the nanometer to millimeter, which can support the reconstruction of centimeter-sized osseous defects has been reported by Fierz et al. [74] to mimic bone. Histological analysis of the scaffolds seeded with osteogenic-stimulated progenitor cells confirmed the suitability of the 3D-printed scaffolds for potential clinical applications.

4 Applications of 3D printed biomaterials

4.1 Tissue engineering

TE is a multidisciplinary field that applies the principles of engineering and life sciences toward the development of biological substitutes [75]. Fundamental to TE is the utilization of living cells to achieve biological substitutes for implantation into the body and/or to foster the remodeling of tissue in some other active manner. Within the field of TE, there are two main approaches that are employed; the first is the use of scaffolds as a cell support to encourage the cells to form their own matrix. The second methodology takes advantage of the scaffold as growth factor or drug-delivery device to induce and aid regeneration inside the body [76]. Key to the use of scaffolds in TE are three main characteristics that the structures should possess [77]. Primarily, the scaffold should be able to mimic the architecture of the native ECM by providing space for vascularization, new tissue formation, and nutrient transport. Additionally, the scaffold should be able to interact with the cellular component to facilitate their activities such as proliferation and differentiation. Finally, the scaffold has to provide a 3D structural support while matching the mechanical properties of native tissues/organs.

Advances in TE have shown to be successful in building a number of tissues that have been used in the clinic such as skin and cornea [78]. However, constructing complex solid organs remains a major physical and biological challenge. Among other challenges are the lack of methods that can simultaneously replicate the tissue micro- and macroarchitecture and methods that can deliver multiple cell types at precise locations. AM has been utilized to try to address these limitations [79] because of its main advantages of precise control and personalized customization [80]. Recently, the term 3D bioprinting has been coined for a specialized class of 3D printing. 3D bioprinting is a layer-by-layer AM technique in which precise positioning of biological materials and living cells [40] can be achieved. In the recent years, the use of 3D bioprinting for manufacturing scaffolds has increased as a result of the benefits of being able to control pore size, shape, and distribution. In addition to this, combined with the ability of CAD manipulation and 3D medical imaging such as CT, 3D bioprinting permits the fabrication of patient-specific constructs [39]. Bone regeneration was one of the first TE applications to take advantage of the technological advances offered via 3D printing of materials [81]. The first scaffolds fabricated for this purpose were manufactured using a biodegradable polymer, namely, poly(caprolactone), and fused deposition modeling as the printing technique (Fig. 5) [80]. The precise



	Design	Build	Accuracy	Design	Build	Accuracy	Design	Build	Accuracy	Design	Build	Accuracy
Pore size (μm)	800	561 ± 10	70 ± 1%	800	636 ± 118	80 ± 15%	400	253 v 44	63 ± 11%	400	279 ± 44	70 ± 11%
Porosity (%)	25	23 ± 1	88 ± 1%	50	46 ± 2	90 ± 2%	25	19 ± 2	76 ± 2%	38	19 ± 3	50 ± 2%
Wall thickness (μm)	500	456 ± 10	91 ± 2%	500	39 ± 11	79 ± 2%	500	403 ± 4	81 ± 1%	500	390 ± 60	78 ± 12%

Fig. 5 3D printing allows the porosity and pore size in scaffolds for systematically studying its effect on bone formation and vascular ingrowth. (Reproduced with permission from M.O. Wang, C.E. Vorwald, M.L. Dreher, E.J. Mott, M.-H. Cheng, A. Cinar, H. Mehdizadeh, S. Somo, D. Dean, E.M. Brey, J.P. Fisher, *Evaluating 3D-printed biomaterials as scaffolds for vascularized bone tissue engineering*, *Adv. Mater.* 27 (2015) 138–144. Copyright (2014) John Wiley and Sons.)

deposition control of 3D printing has facilitated the study of the effect of porosity and pore size on bone ingrowth and vascularization, allowing to create the most adequate scaffolds for host integration [82].

Many different materials have been 3D printed for manufacturing these scaffolds, among them are synthetic polyesters (i.e., PEG-PLA, PCL, etc.), natural polymers (i.e., alginate, chitosan, gelatine, etc.), ceramic composites (i.e., calcium phosphate and hydroxyapatite), and combinations of them [83]. A noteworthy example of the 3D printed combination materials is the hyperplastic “bone” scaffold, which is composed of 90 wt% hydroxyapatite and 10 wt% poly(caprolactone) or poly(lactic-co-glycolic acid) [84]. These scaffolds became rapidly vascularized and showed and osteoregenerative properties when implanted in vivo. Khalyfa et al. have also reported [85] a highly bio-compatible calcium phosphate powder-binder, which has been used to produce porous medical implants such as scaffolds for cranial reconstruction (Fig. 6A). Another example of a 3D bioprinting for TE application is cardiac regeneration. Tissue-engineered heart valve conduits have been fabricated using 3D bioprinting and reported by Duan et al. [86] The trileaflet valve conduits were bioprinted using a combination of methacrylate-functionalized hyaluronic acid and methacrylate-functionalized gelatine with encapsulated human aortic valve interstitial cells. Prevascularized stem cell patches have also been bioprinted for promoting cardiac repair [87]. In in vivo studies, these patches exhibited

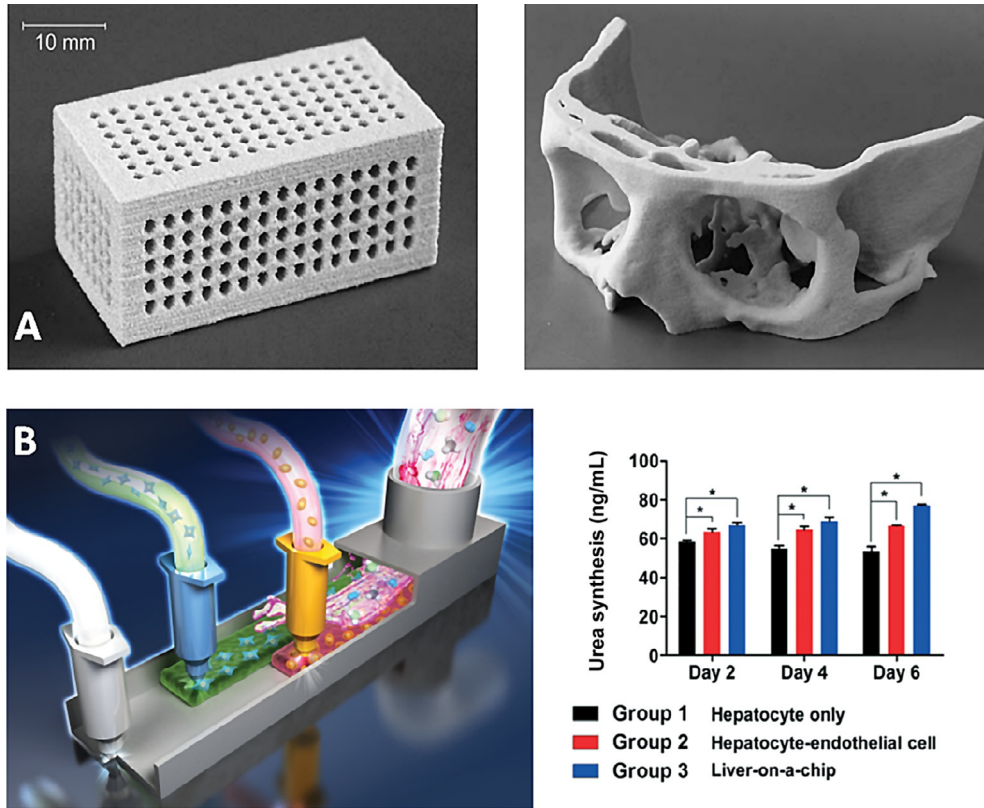


Fig. 6 Representation of different applications of 3D bioprinting in tissue engineering. (A) 3-D printed proof-of-concept cuboid structure and structurally complex cranial structure. (B) Liver on a chip manufactured with 3 different biomaterials and 2 different cell types. ((A) Reproduced with permission from A. Khalyfa, S. Vogt, J. Weisser, G. Grimm, A. Rechtenbach, W. Meyer, M. Schnabelrauch, *Development of a new calcium phosphate powder-binder system for the 3D printing of patient specific implants*, *J. Mater. Sci. Mater. Med.* 18 (2007) 909–916. (B) Reproduced from H. Lee, D.-W. Cho, *One-step fabrication of an organ-on-a-chip with spatial heterogeneity using a 3D bioprinting technology*, *Lab Chip* 16 (2016) 2618–2625 with permission from the Royal Society of Chemistry.)

enhanced cardiac functions, reduced cardiac hypertrophy, and increased migration of cells from patch to the infarct area. Liver microtissues used for drug testing and disease modeling are another example of 3D bioprinted TE constructs. Faulker-Jones et al. have reported [88] the fabrication of functional mini livers using human induced pluripotent stem cells encapsulated in an alginate hydrogel matrix and deposited with a microvalve printer. The human liver is a very complex organ, highly vascularized and composed of many different cell types. This kind of complexity cannot be easily reproduced in vitro, but using the versatility of 3D printing Lee et al. designed [89] a one-step method for

fabricating an organ on a chip that can tackle this complexity. The artificial liver was fabricated with a microfluidic system with multiple cell types and biomaterials, which showed that hepatocytes cultured in this system had increased liver function when compared with the ones cultured with standard static methods (Fig. 6B).

4.2 Medicine and drug delivery

The use of AM for medical applications and drug delivery has grown rapidly in the previous decade. [90] In the medical field, 3D printing can be used for surgical planning, medical education, and customized implant design [91]. The combination of AM and advanced medical imaging enables the creation of patient-specific implants and the reproduction of the complex architecture of tissues. [92] Combining 3D printing with advanced medical imaging, a suite of techniques including the use of CT or MRI in combination with postprocessing tools and algorithms [93], a range of medical implants have been 3D printed for a variety of applications, including heart valves [86], ears [94], articular surface [95], meniscus [96], trachea splint [97], bone [98], cranium [99], and mandible [100] to name but a few. The postprocessing tools used in advanced medical imaging allow a series of 2D images to be converted into a 3D view or model of the anatomy [101]. After the imaging data are acquired, they are then saved in DICOM (digital imaging and communications in medicine) format. The DICOM files are then manipulated using 3D postprocessing tools, which usually include thresholding, segmentation, sculpting, trimming, and smoothing tools. The contours of a segmented region of interest can be computationally transformed into a 3D triangle mesh. The mesh data then are further processed using CAD software where additional smoothing and editing is performed to finally generate a 3D STL (stereolithography) file, which is compatible with 3D printer software [102]. This combination of techniques has allowed for custom-designed and personalized implants and scaffolds to be produced quickly and effectively.

Otology, or the study of the anatomy and diseases of the ear, is one of the first medical fields that explored 3D printing as a manufacturing method for implants and devices to be produced. The hearing aid industry has already transitioned its entire operations to the use of 3D printing [103]. Since the implementation of 3D printing technology in this field, more than 10 million hearing aid shells have already been manufactured using 3D printers. Currently, EnvisionTEC has nine different biocompatible polymers that have been developed specially for hearing aids, most of them strong, though, water-resistant photocrosslinked polymers [104]. 3D printing has reduced the hearing aid manufacturing process to three steps: scanning, modeling, and printing. As a result of this new technology, hundreds of thousands of custom-made products are able to be produced en masse every year [105].

The concept of personalized medicine has also driven the use of 3D printing in pharmaceutical drug delivery. Compared to the traditional pharmaceutical product

manufacturing process, 3D printing offers several advantages such as specific dosage to each patient needs, reduction of materials wastage, and amenability to broad types of pharmaceutical active ingredients, including poorly water-soluble peptides and proteins [106]. Examples of 3D printed pharmaceutical formulations include guaifenesin tables [107], levofloxacin implants [108], rifampicin nanoparticles [109], and a folic acid nanosuspension [110].

4.3 Dentistry

Digital dentistry and AM are rapidly transforming the dental industry and now 3D printing is used for a wide range of dental applications, including dental and orthodontics models, direct crowns and bridges, dental aligners, night guards, surgical drill guides, flexible gingiva masks, and denture bases (Fig. 7) [111]. Using AM methods for the fabrication of dental models is an approach that has increasingly been employed for surgical planning, simulation, and orthodontics. Studies have compared the models manufactured with 3D printing techniques with those made with the traditional plaster method and revealed that the 3D printed constructs are clinically acceptable in terms of accuracy and reproducibility [112]. The advantages of using AM techniques instead of the traditional method arise from the ability to use digital models to fabricate patient-specific designs, which increase the efficiency of manufacture and improved comfort for the patient.

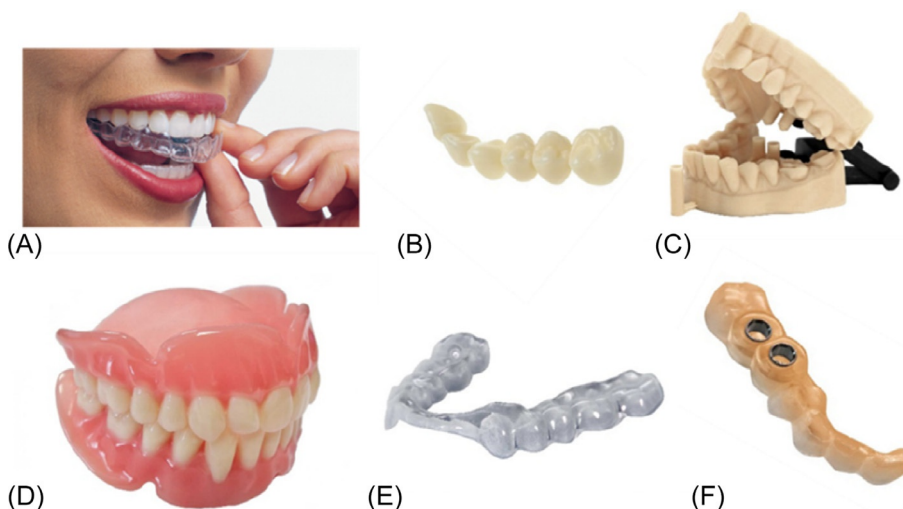


Fig. 7 Current dental applications of 3D printing. (A) Invisalign® dental aligners, (B) bridges (E-DENT 400C&B MHF), (C) dental and orthodontic models (E-MODEL), (D) denture bases (E-DENTURE), (E) night guards (E-GUARD), and (F) surgical guides (E-GUIDE). (Images from B–F were reproduced with permission from EnvisionTEC.)

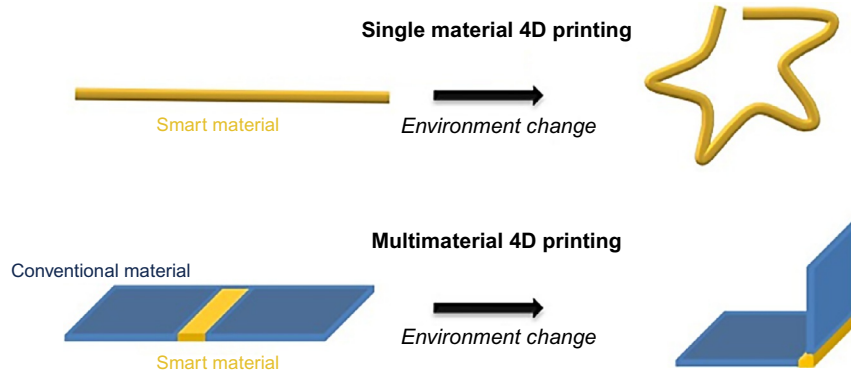
Fabrication of dental aligners using 3D printing has completely transformed the orthodontics treatment. The company Invisalign[®] uses digital dentistry and SLA technology to manufacture approximately 220,000 aligners per day, and almost 8 million per year [113]. 3D printing enables each set to be personalized easily to individual patient-specific needs [114]. The material used for fabricating these aligners can include styrenic block copolymers, silicone rubbers, elastomeric alloys, thermoplastic elastomers, thermoplastic vulcanizate elastomers, polyurethane elastomers, block copolymer elastomers, polyolefin blend elastomers, and thermoplastic copolyester elastomers [115]. The main advantages of these devices over conventional aligners or braces are their improved aesthetics, increased comfort to wear, and improved oral hygiene as a result of the device being removable [116].

3D printing has also been used for aiding periodontal repair. Rasperini et al. [117] have reported the first in-human case treatment of a large periodontal osseous defect using a 3D printed patient-specific scaffold loaded with growth factors. The scaffolds were 3D printed using selective laser sintering technologies and poly(caprolactone) containing 4 wt% hydroxyapatite. The internal part of the scaffold had a reservoir for storing a human recombinant platelet-derived growth factor. The study reported that after 12 months of in vivo implantation the scaffold remained intact; however, the growth factor release kinetics required further optimization.

5 4D printing and its applications for biomaterials

4D printing is a novel technology, which is pushing the boundaries of traditional AM techniques. Unlike conventional 3D printing that only provides the user the freedom of controlling the shape of the product, the concept of 4D printing introduces another dimension, time, into the 3D structure. Momeni et al. [118] described such a process as: “A targeted evolution of 3D printed structure, in terms of shape, property and functionality,” and therefore the final geometry or property of the 3D printed construct can vary under different situations and in different time frames.

Although many definitions for 4D printing have been proposed, here the process is described as “the use of a 3D printer to print objects which could change or alter their shape after the manufacturing; such a change could be taken place due to many factors such as air, heat and other chemical reactions caused due to materials used in the manufacturing of these object[s]” as defined by Ramesh et al. [119] Khoo et al. further categorized 4D printing into single-material 4D printing and multimaterial 4D printing (Scheme 2) [120]. Both methodologies rely on smart materials that can exhibit different geometry or functional performance under a range of conditions such as pH [121], or temperature [122,123]. However, the multimaterial approach possesses increased flexibility in the number and class of material available and as a result has access to wider applications. It facilitates the user to not only use different smart materials, but also these



Scheme 2 Schematic of two routines that smart materials are used for manufacturing 4D printed smart devices.

materials in combination with a “conventional” material, to achieve designed performance under different conditions. This capability significantly increases the number of applicable materials suitable for the 4D printing process. However, as traditional materials do not possess the ability to react or translate in response to an external environmental change, such a methodology may require extra design consideration with respect to the distribution of different materials within the construct to achieve the desired performance or translation over time.

As a wider pallet of materials and applications are accessible using the multimaterial approach to 4D printing, this section will focus solely on this class of 4D constructs. Furthermore, the American Society for Testing and Materials (ASTM) categorizes conventional 3D print techniques into seven distinct groups, within which material jetting and material extrusion are the two key techniques, which have found use in AM of multimaterials. It is thus not surprising that these two techniques have also been exploited in the field of 4D printing to the greatest extent. It should be noted that other techniques such as stereolithographic and selective laser sintering can also be used to fabricating multimaterial objects via 3D printing; however, these methods become increasingly complicated when switching materials during the printing process.

5.1 Techniques in 4D printing

Material extrusion or extrusion printing is a technique in which a paste or molten materials are forced through a nozzle by screw or compressed air to form a filament of material, which is easily deposited and solidifies rapidly post printing. The size of the nozzle is directly related to the diameter of the extruded filament, and therefore the resolution of the objects fabricated from such a method is of a similar scale, approximately as low as one hundred of microns. By integrating independent printheads for use with multiple different materials, multimaterial structures can be produced by selectively

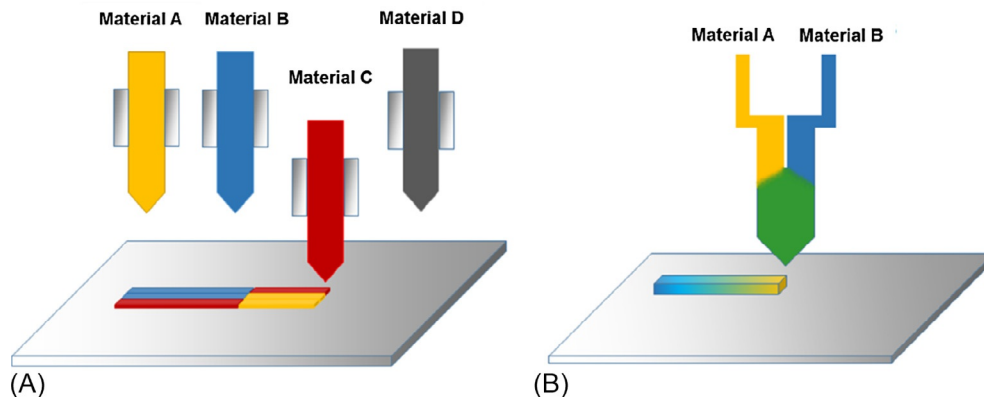


Fig. 8 Schematic of the two multimaterial extrusion methods: (A) Multimaterial extrusion printer based on different printheads and independent feedstocks. (B) Multimaterial extrusion printer based on shared printhead and independent feedstock.

depositing the desired material as required (Fig. 8A). The number of materials that can be included in a single structure will also increase as more printhead and feedstocks are integrated into the printer [124, 125]. The bioprinter from Aether©, for example, has demonstrated the capability of integrating up to 10 different printheads inside one printer, thus allowing fabrication of highly complex and intricate structures.

To achieve a gradient multimaterial composite with higher resolution, a slightly modified printhead is introduced (Fig. 8B), in which different materials can enter a mixing chamber before extrusion. By controlling the input volume ratio of materials A and B, a range of different composite materials can be produced by using only a few input materials [59].

Jetting techniques have been recognized as one of the most well-established technologies for fabricating multimaterial components [120]. During the material jetting or inkjet printing process, formulations are ejected from the printhead as a series of individual, of picoliter volume, droplets. Layers of material are subsequently deposited on the substrate and combined to form three-dimensional structures. By introducing multiple printheads containing different materials, the composition of the printed structure can be altered (Fig. 9A) to fabricate a variety of composite materials. As such, the composition can be manipulated at the single droplet level ($\sim 30\ \mu\text{m}$, Fig. 9B), and therefore fine tuning of the functionality of the printed structure can be controlled by changing the density and distribution of different materials at targeted locations. In comparison to 3D objects printed via the extrusion method, printing using material jetting technologies allows access to structures with higher feature resolution ($80\ \mu\text{m}$ vs. $100\text{--}200\ \mu\text{m}$ for extrusion printing). Although the resolution of the printed structures is improved, inkjet-based methodologies require strict operating and materials parameters to be observed such as

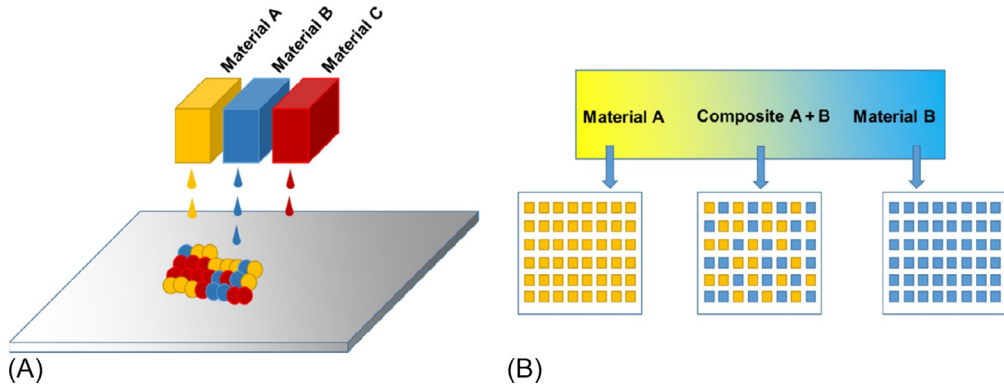


Fig. 9 (A) Schematic of multimaterial jetting technique: multimaterial structure was achieved by coprint of different materials from different printheads and (B) schematic of how a range of polymer composite was formed by controlling the distribution different materials.

material viscosity (normally between 1 and 30 mPa s), and thus the applicable materials are limited when compared with material extrusion technologies.

Despite the prevalence of material extrusion and material jetting techniques in 4D printing technologies, other 3D print methodologies have been utilized to produce responsive multimaterial structures. In 2006, Inamdar et al. demonstrated [126] the use of a multivat SLA system with different resins located in each vat to produce multimaterial structures (Fig. 10A). Chen and Zhang [127] have also described the use of SLA with integrated an automatic material feeding and cleaning system to sequentially fill the resin vat with different materials to achieve multimaterial structures (Fig. 10B). Both methods require cleaning steps when switching building material in order to minimize

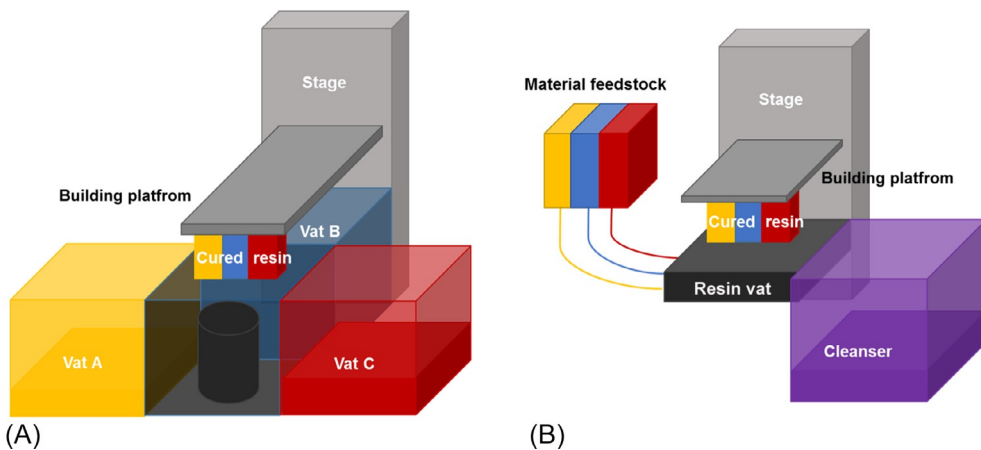


Fig. 10 Schematic of the two multimaterial stereolithography techniques: (A) multivat stereolithography and (B) single vat with multimaterial feed stock technique.

crosscontamination and exert control of material composition, As a result, the overall production sequence is complex and time consuming. Other fabrication methods such as laser sintering [128] or laser melting [129] with controlled distribution of powders within the build space have been trialed to form multimaterial objects. The integration of material extrusion techniques with SLA to deposit different materials [130] has also been attempted although both methodologies are not widely used as a result of fabrication limitations.

5.2 Materials and applications of biomaterials in 4D

Smart hydrogels are a varied group of materials that have excellent potential in biomedical or bioengineering applications. Hydrogels are normally recognized as having similar properties to natural tissues, amenable to environment change, biocompatible, and easily modified [119]. Many of the smart hydrogel structures used for 4D printing process rely on manipulating the hydrogel geometry through controlling the swelling ratio of the structure. The swelling ratio can be controlled by introducing isotropic fibers or designing the molecular structures to achieve different swelling in response to environment stimuli such as pH, temperature, electric field [131], and induce geometry translations accordingly.

Synthetic hydrogens such as those comprising polymeric materials have been widely reported. For example, Dutta and Cohn [132] have prepared a poly(ethylene oxide)-poly(propylene oxide)-poly(ethylene oxide) triblock copolymer with methacrylate functionality which underwent gelation in water. The material exhibited fast and crucially reversible swelling at different pH's and temperatures. Using SLA, a 3D structure was successfully produced. Han et al. [133] have reported the use of poly(ethylene glycol) co-polymerized with acrylic acid to achieve a hydrogel that can exhibit reversible deformation in the presence of an electronic field. The deformation was induced by the presence of ionized carboxylic groups within the hydrogel structure that resulted in variation of the osmotic pressure in the network. Through SLA methods, 3D printed smart hydrogels structures were produced that can undergo movement by controlling the electronic field in close proximity to the object.

Composites have also found significant use in 4D printing applications. Gladman et al. [134] have prepared smart hydrogels containing a soft acrylamide matrix embedded with stiff cellulose fibrils, which mimics the composition of plant cell walls. When the hydrogel swelling in water environment, the aligned fiber structure will restrict the deformation and therefore cause anisotropic swelling. By incorporating digital design and 4D print, they produced structures that can self-assemble into designed geometry in water environment. Moreover, Xiong et al. [135] have reported in their recent publication the use of hydrogel-containing magnetic particles for preparing smart hydrogels. Fe₃O₄ nanoparticles were formulated into an aqueous solution of poly(ethylene glycol)

di-acrylate and cured by nanoscale SLA technique (two-photon) to prepare smart 4D hydrogel structures. Conformational changes within the hydrogel were subsequently induced through the application of a magnetic field.

Shape memory polymers are a group of materials that has found popularity in biomedical applications. In 2002, both Lendlein and Langer [136], and El Feninat et al. [137] stated the potential of using biodegradable, elastic shape memory polymers for biomedical applications, respectively. A number of other proof-of-concept studies have demonstrated the use of shape memory polymers as catheters [138], stents [139], and surgical sutures [136]. To effectively make use of shape memory polymers in 4D printing, two elements are required, namely, these are a crosslinking point and switchable segments [140]. The crosslinking point could be either a covalent bond or physical/mechanical bond that fixes the polymer chains together, while the switchable segments may comprise a polymer moiety, which can be “activated” by passing through a thermal transition such as glass transition or melting. The printed structures (original shape) can be programmed into a temporary shape when heated above a thermal transition temperature. The transition temperatures for each material may be tuned by using polymer segments with different glass transition temperatures, for example. To reverse the process, the temporary shape can once again be heated to its transition temperature, allowing the original structure to be formed once again.

Generally, materials, which are selected for shape memory 4D printing, are biopolymers featuring acrylate or methacrylate moieties. Photopolymerization is a method to quickly create a polymer network, which is constructed of covalent bonds. Moreover, it is also one of the most important chemical reactions that have been widely used in 3D print techniques such as material extrusion, material ink jetting, and SLA as described in Section 2. Biomaterials such as poly(caprolactone) and poly(ethylene glycol), which have been chemically modified to enable UV curing, are therefore strong candidates for 4D printing applications. Zarek et al. [141] demonstrated the use of a poly(caprolactone) precursor with methacrylate moieties to manufacture a self-assembled device for personalized endoluminal applications. Hot melt SLA was used to create customized tracheal stents that could expand and anchor itself after placement to prevent stent migration or stent fracture. López-Valdeolivas et al. [123] reported a diacrylate liquid crystal polymer precursor, which exhibited a thermoresponsive and reversible shape-morphing behavior upon photocuring. It was suggested that this material could be used as an actuator or smart device in medicine applications. Furthermore, Yakacki et al. [139] demonstrated the use of bis-acrylate terminated poly(ethylene glycol) with different molecular weights to produce shape memory structures and claimed the potential application in stent manufacturing. More recently, Ge et al. [142] have described a bis-acrylate terminated poly(ethylene glycol) structure afforded through microstereolithography techniques. The resulting 3D printed material was used to manufacture a shape memory stent that can be deformed and then return to the original geometry at an elevated temperature.

6 Conclusions and future perspectives

6.1 3D printed biomaterials

Biomaterials and biofabrication have a unique set of requirements, which must be upheld in order to achieve the desired function or application for the construct. Through the use of AM, advancements have been made in many key areas such as complexity, customization, cost-effective production, and ease of access [42]. 3D bioprinting promises solutions to some of the most challenging hurdles in the field of biomedical science, including TE, dentistry, and drug-delivery systems by creating complex architectures. However, the most significant obstacles to the advancement of 3D bioprinting technologies are perhaps the lack of viable bioinks and biocompatible materials. Traditional single-component formulations lack one or more of the characteristics desired in a bioink, including high structural fidelity and printability, high mechanical strength postprinting, and bioactivity and biodegradability. Increasing crosslink density of polymers, in an attempt to enhance the mechanical and rheological deficiencies of bioinks, tends to reduce the cytocompatibility of single-component formulations. Recent developments in advanced bionics avoid these tradeoffs without sacrificing cell viability. In time, 3D printing will allow the development of new biomedical implants, engineered tissues and organs and find use in controlled and personalized drug-delivery systems [143]. The flexibility offered by AM also allows for complex shapes and geometries to be engineered from multimaterials, which are not easily accessed through traditional manufacturing techniques [144]. Patient-specific needs will also be addressed through customizable designs, drug dose, and release profiles; allowing healthcare to be tailored to individual needs [145–147]. Moreover, AM will find applications in planning of surgeries, improving their efficiencies and effectiveness while reducing further procedures, which may be required to adapt implants to the patient [148]. Cost benefits may also be observed through the use of AM techniques. Prototyping of parts will become less time consuming and small productions volumes, which are typical in the biomedical industry, may become more cost effective with minimal material wastage and faster build times when compared to traditional manufacturing techniques [90]. Perhaps the most exciting innovation will be the open access of information. 3D printers are no longer confined to the laboratory and easy access to CAD files, such as via the National Institutes of Health project: *3D Print Exchange*, will allow for ideas and designs to be shared among researchers and the general public. This information sharing will broaden the scope of 3D printing and allow for ideas and designs to be readily shared to further progress the field of biomaterials, ultimately finding use in modern society.

6.2 4D printed biomaterials

4D printing as an advanced manufacturing technique opens a new era in manufacturing of smart devices for biomedical or bioengineering application that has subverted people's

understanding in device design and manufacturing. It provides the user with opportunities to designing a dynamic structure that can be programmed and exhibit desired functionality in different situations. Although traditional single-material 3D printing techniques can be used for processing smart materials for such 4D print concept, the trends of 4D printing are using those techniques that can produce devices that contain more than one material such as inkjet printing or extrusion. This will provide the user the ability to either combine different smart materials or use smart materials in collaboration with conventional materials to achieve devices with more complex functionality.

Although 4D printing has already shown enormous potentials in different areas, it is still in an early stage of development and requires further investigation to unlock the full potential of this technique. The development of 4D printing will require close interdisciplinary collaboration between such fields as materials chemistry and engineering. One of the key challenges for 4D printing is the availability of smart biomaterials that can be used to drive the spatial conformation of the device while exposed to a desired environment stimulus. Current research is predominantly focused on either shape memory materials or smart hydrogels, but as the research momentum increases in this interdisciplinary field, more breakthroughs are envisaged that will help expand the smart 4D printing materials database.

Acknowledgments

The authors would like to acknowledge funding from the EPSRC (EP/N024818/1) support of a postdoctoral fellowships for LRH, YH, LRC, and ZZ.

References

- [1] C.M.B. Ho, S.H. Ng, Y.J. Yoon, A review on 3D printed bioimplants, *Int. J. Precis. Eng. Manuf.* 16 (2015) 1035–1046.
- [2] J.S. Miller, J.A. Burdick, Editorial: special issue on 3D printing of biomaterials, *ACS Biomater. Sci. Eng.* 2 (2016) 1658–1661.
- [3] R.L. Truby, J.A. Lewis, Printing soft matter in three dimensions, *Nature* 540 (2016) 371–378.
- [4] R.D. Farahani, M. Dubé, D. Therriault, Three-dimensional printing of multifunctional nanocomposites: manufacturing techniques and applications, *Adv. Mater.* 28 (2016) 5794–5821.
- [5] C. Sun, N. Fang, D.M. Wu, X. Zhang, Projection micro-stereolithography using digital micro-mirror dynamic mask, *Sens. Actuators A Phys.* 121 (2005) 113–120.
- [6] S. Kawata, H.B. Sun, T. Tanaka, K. Takada, Finer features for functional microdevices, *Nature* 412 (2001) 697–698.
- [7] R.A.L. Jones, *Soft Condensed Matter*, Oxford Univ. Press, 2002, pp. 73–93.
- [8] N.B. Palaganas, J.D. Mangadlao, A.C.C. De Leon, J.O. Palaganas, K.D. Pangilinan, Y.J. Lee, R.C. Advincula, 3D printing of photocurable cellulose nanocrystal composite for fabrication of complex architectures via stereolithography, *ACS Appl. Mater. Interfaces* 9 (2017) 34314–34324.
- [9] A. Chiappone, E. Fantino, I. Roppolo, M. Lorusso, D. Manfredi, P. Fino, C.F. Pirri, F. Calignano, 3D printed PEG-based hybrid nanocomposites obtained by sol-gel technique, *ACS Appl. Mater. Interfaces* 8 (2016) 5627–5633.

- [10] S. Shin, H. Kwak, J. Hyun, Melanin nanoparticle-incorporated silk fibroin hydrogels for the enhancement of printing resolution in 3D-projection stereolithography of poly(ethylene glycol)-tetraacrylate bio-ink, *ACS Appl. Mater. Interfaces*. 10 (2018) 23573–23582.
- [11] L. Deng, Y. Deng, K. Xie, AgNPs-decorated 3D printed PEEK implant for infection control and bone repair, *Colloids Surf. B Biointerfaces* 160 (2017) 483–492.
- [12] J. Yu, Y. Xu, S. Li, G.V. Seifert, M.L. Becker, Three-dimensional printing of nano hydroxyapatite/poly(ester urea) composite scaffolds with enhanced bioactivity, *Biomacromolecules* 18 (2017) 4171–4183.
- [13] Y.C. Chou, W.L. Yeh, C.L. Chao, Y.H. Hsu, Y.H. Yu, J.K. Chen, S.J. Liu, Enhancement of tendon-bone healing via the combination of biodegradable collagen-loaded nanofibrous membranes and a three-dimensional printed bone-anchoring bolt, *Int. J. Nanomed.* 11 (2016) 4173–4186.
- [14] N.H.A. Ngadiman, N.M. Yusof, A. Idris, E. Fallahiazouard, D. Kurniawan, Novel processing technique to produce three dimensional polyvinyl alcohol/maghemite nanofiber scaffold suitable for hard tissues, *Polymers (Basel)* 10 (2018) 1–18.
- [15] N. Maurmann, D.P. Pereira, D. Burguez, A. Di Luca, A. Longoni, G. Criscenti, Cryogenic 3D printing for producing hierarchical porous and rhBMP-2-loaded Ca-P/PLLA nanocomposite scaffolds for bone tissue engineering, *Biofabrication* 9 (2017). 025031(1)–025031(13).
- [16] X. Zhai, Y. Ma, C. Hou, F. Gao, Y. Zhang, C. Ruan, H. Pan, W.W. Lu, W. Liu, 3D-printed high strength bioactive supramolecular polymer/clay nanocomposite hydrogel scaffold for bone regeneration, *ACS Biomater. Sci. Eng.* 3 (2017) 1109–1118.
- [17] S.A. Wilson, L.M. Cross, C.W. Peak, A.K. Gaharwar, Shear-thinning and thermo-reversible nanoengineered inks for 3D bioprinting, *ACS Appl. Mater. Interfaces* 9 (2017) 43449–43458.
- [18] Y. Gu, X. Chen, J.H. Lee, D.A. Monteiro, H. Wang, W.Y. Lee, Inkjet printed antibiotic- and calcium-eluting bioresorbable nanocomposite micropatterns for orthopedic implants, *Acta Biomater.* 8 (2012) 424–431.
- [19] L.R. Hart, S. Li, C. Sturgess, R. Wildman, J.R. Jones, W. Hayes, 3D printing of biocompatible supramolecular polymers and their composites, *ACS Appl. Mater. Interfaces*. 8 (2016) 3115–3122.
- [20] S. Nganga, N. Moritz, R. Kolakovic, K. Jakobsson, J.O. Nyman, M. Borgogna, A. Travan, M. Crosera, I. Donati, P.K. Vallittu, N. Sandler, Inkjet printing of Chitlac-nanosilver—a method to create functional coatings for non-metallic bone implants, *Biofabrication* 6 (2014). 041001(1)–041001(7).
- [21] S.F.S. Shirazi, S. Gharekhani, M. Mehrali, H. Yarmand, H.S.C. Metselaar, N. Adib Kadri, N.A.A. Osman, A review on powder-based additive manufacturing for tissue engineering: selective laser sintering and inkjet 3D printing, *Sci. Technol. Adv. Mater.* 16 (2015) 033502.
- [22] I. Tolosa, F. Garciandía, F. Zubiri, F. Zapirain, A. Esnaola, Study of mechanical properties of AISI 316 stainless steel processed by “selective laser melting”, following different manufacturing strategies, *Int. J. Adv. Manuf. Technol.* 51 (2010) 639–647.
- [23] E. Yasa, J. Deckers, J. Kruth, The investigation of the influence of laser re-melting on density, surface quality and microstructure of selective laser melting parts, *Rapid Prototyp. J.* 17 (2011) 312–327.
- [24] B. Vandenbroucke, J.P. Kruth, Selective laser melting of biocompatible metals for rapid manufacturing of medical parts, *Rapid Prototyp. J.* 13 (2007) 196–203.
- [25] C. Sanz, V. García Navas, Structural integrity of direct metal laser sintered parts subjected to thermal and finishing treatments, *J. Mater. Process. Technol.* 213 (2013) 2126–2136.
- [26] J. Kruth, P. Mercelis, J. Van Vaerenbergh, L. Froyen, M. Rombouts, Binding mechanisms in selective laser sintering and selective laser melting, *Rapid Prototyp. J.* 11 (2005) 26–36.
- [27] A.B. Spierings, N. Herres, G. Levy, Influence of the particle size distribution on surface quality and mechanical properties in AM steel parts, *Rapid Prototyp. J.* 17 (2011) 195–202.
- [28] A.B. Spierings, T.L. Starr, K. Wegener, Fatigue performance of additive manufactured metallic parts, *Rapid Prototyp. J.* 19 (2013) 88–94.
- [29] L. Zhang, J. Wang, Effect of temperature and loading mode on environmentally assisted crack growth of a forged 316L SS in oxygenated high-temperature water, *Corros. Sci.* 87 (2014) 278–287.
- [30] T.F. Kong, L.C. Chan, T.C. Lee, Experimental study of effects of process parameters in forge-welding bimetallic materials: AISI 316L stainless steel and 6063 aluminium alloy, *Strain* 45 (2009) 373–379.

- [31] J. Delgado, J. Ciurana, C.A. Rodríguez, Influence of process parameters on part quality and mechanical properties for DMLS and SLM with iron-based materials, *Int. J. Adv. Manuf. Technol.* 60 (2012) 601–610.
- [32] R. Li, J. Liu, Y. Shi, M. Du, Z. Xie, 316L stainless steel with gradient porosity fabricated by selective laser melting, *J. Mater. Eng. Perform.* 19 (2010) 666–671.
- [33] D. Chimene, K.K. Lennox, R.R. Kaunas, A.K. Gaharwar, Advanced bioinks for 3D printing: a materials science perspective, *Ann. Biomed. Eng.* 44 (2016) 2090–2102.
- [34] H.N. Chia, B.M. Wu, Recent advances in 3D printing of biomaterials, *J. Biol. Eng.* 9 (2015). 4(1)–4(14).
- [35] D. Herzog, V. Seyda, E. Wycisk, C. Emmelmann, Additive manufacturing of metals, *Acta Mater.* 117 (2016) 371–392.
- [36] S.C. Ligon, R. Liska, J. Stampfl, M. Gurr, R. Mühlaupt, Polymers for 3D printing and customized additive manufacturing, *Chem. Rev.* 117 (2017) 10212–10290.
- [37] R.F. Pereira, P.J. Bartolo, Manufacturing of advanced biodegradable polymeric components, *J. Appl. Polym. Sci.* 132 (2015). 42458(1)–42458(15).
- [38] W. Zhu, X. Ma, M. Gou, D. Mei, K. Zhang, S. Chen, 3D printing of functional biomaterials for tissue engineering, *Curr. Opin. Biotechnol.* 40 (2016) 103–112.
- [39] F.P.W. Melchels, M.A.N. Domingos, T.J. Klein, J. Malda, P.J. Bartolo, D.W. Huttmacher, Additive manufacturing of tissues and organs, *Prog. Polym. Sci.* 37 (2012) 1079–1104.
- [40] S.V. Murphy, A. Atala, 3D bioprinting of tissues and organs, *Nat. Biotechnol.* 32 (2014) 773–785.
- [41] X. Wang, M. Jiang, Z. Zhou, J. Gou, D. Hui, 3D printing of polymer matrix composites: a review and prospective, *Compos. B Eng.* 110 (2017) 442–458.
- [42] T.D. Ngo, A. Kashani, G. Imbalzano, K.T.Q. Nguyen, D. Hui, Additive manufacturing (3D printing): a review of materials, methods, applications and challenges, *Compos. B* 143 (2018) 172–196.
- [43] T. Duda, L.V. Raghavan, 3D metal printing technology, *IFAC-Pap. Online* 49 (2016) 103–110.
- [44] H.D. Carlton, A. Haboub, G.F. Gallegos, D.Y. Parkinson, A.A. MacDowell, Damage evolution and failure mechanisms in additively manufactured stainless steel, *Mater. Sci. Eng. A.* 651 (2016) 406–414.
- [45] G. Casalino, S.L. Campanelli, N. Contuzzi, A.D. Ludovico, Experimental investigation and statistical optimisation of the selective laser melting process of a maraging steel, *Opt. Laser Technol.* 65 (2015) 151–158.
- [46] L.E. Murr, E. Martinez, J. Hernandez, S. Collins, K.N. Amato, S.M. Gaytan, P.W. Shindo, Microstructures and properties of 17–4 PH stainless steel fabricated by selective laser melting, *J. Mater. Res. Technol.* 1 (2012) 167–177.
- [47] J. Mazumder, J. Choi, K. Nagarathnam, J. Koch, D. Hetzner, The direct metal deposition of H13 tool steel for 3-D components, *JOM.* 49 (1997) 55–60.
- [48] D. Kong, X. Ni, C. Dong, X. Lei, L. Zhang, C. Man, J. Yao, X. Cheng, X. Li, Bio-functional and anti-corrosive 3D printing 316L stainless steel fabricated by selective laser melting, *Mater. Des.* 152 (2018) 88–101.
- [49] R. Bibb, D. Eggbeer, R. Williams, Rapid manufacture of removable partial denture frameworks, *Rapid Prototyp. J.* 12 (2006) 95–99.
- [50] L.E. Murr, K.N. Amato, S.J. Li, Y.X. Tian, X.Y. Cheng, S.M. Gaytan, E. Martinez, P.W. Shindo, F. Medina, R.B. Wicker, Microstructure and mechanical properties of open-cellular biomaterials prototypes for total knee replacement implants fabricated by electron beam melting, *J. Mech. Behav. Biomed. Mater.* 4 (2011) 1396–1411.
- [51] S. Amin Yavari, L. Loozen, F.L. Paganelli, S. Bakhshandeh, K. Lietaert, J.A. Groot, A.C. Fluit, C.H.E. Boel, J. Alblas, H.C. Vogely, H. Weinans, A.A. Zadpoor, Antibacterial behavior of additively manufactured porous titanium with nanotubular surfaces releasing silver ions, *ACS Appl. Mater. Interfaces* 8 (2016) 17080–17089.
- [52] P. Habibovic, U. Gbureck, C.J. Doillon, D.C. Bassett, C.A. van Blitterswijk, J.E. Barralet, Osteoconduction and osteoinduction of low-temperature 3D printed bioceramic implants, *Biomaterials* 29 (2008) 944–953.
- [53] U. Gbureck, T. Hölzel, C.J. Doillon, F.A. Müller, J.E. Barralet, Direct printing of bioceramic implants with spatially localized angiogenic factors, *Adv. Mater.* 19 (2007) 795–800.

- [54] S. Tarafder, W.S. Dernell, A. Bandyopadhyay, S. Bose, SrO- and MgO-doped microwave sintered 3D printed tricalcium phosphate scaffolds: mechanical properties and in vivo osteogenesis in a rabbit model, *J. Biomed. Mater. Res. B Appl. Biomater.* 103 (2015) 679–690.
- [55] H. Seyednejad, D. Gawlitta, R.V. Kuiper, A. De Bruin, C.F. Van Nostrum, T. Vermonden, W.J.A. Dhert, W.E. Hennink, In vivo biocompatibility and biodegradation of 3D-printed porous scaffolds based on a hydroxyl-functionalized poly(ϵ -caprolactone), *Biomaterials* 33 (2012) 4309–4318.
- [56] T. Patrício, M. Domingos, A. Gloria, U. D'Amora, J.F. Coelho, P.J. Bártolo, Fabrication and characterisation of PCL and PCL/PLA scaffolds for tissue engineering, *Rapid Prototyp. J.* 20 (2014) 145–156.
- [57] C. Sturgess, C.J. Tuck, I.A. Ashcroft, R.D. Wildman, 3D reactive inkjet printing of polydimethylsiloxane, *J. Mater. Chem. C* 5 (2017) 9733–9745.
- [58] M.N. Cooke, J.P. Fisher, D. Dean, C. Rimnac, A.G. Mikos, Use of stereolithography to manufacture critical-sized 3D biodegradable scaffolds for bone ingrowth, *J. Biomed. Mater. Res. B Appl. Biomater.* 64 (2003) 65–69.
- [59] S. Matsumura, A.R. Hlil, C. Lepiller, J. Gaudet, D. Guay, Z. Shi, S. Holdcroft, A.S. Hay, Ionomers for proton exchange membrane fuel cells with sulfonic acid groups on the end-groups: novel branched poly(ether-ketone)s, *Am. Chem. Soc. Polym. Prepr. Div. Polym. Chem.* 49 (2008) 511–512.
- [60] M.S. Hahn, L.J. Taite, J.J. Moon, M.C. Rowland, K.A. Ruffino, J.L. West, Photolithographic patterning of polyethylene glycol hydrogels, *Biomaterials* 27 (2006) 2519–2524.
- [61] T. Billiet, E. Gevaert, T. De Schryver, M. Cornelissen, P. Dubruel, The 3D printing of gelatin methacrylamide cell-laden tissue-engineered constructs with high cell viability, *Biomaterials* 35 (2014) 49–62.
- [62] R. Gauvin, Y.C. Chen, J.W. Lee, P. Soman, P. Zorlutuna, J.W. Nichol, H. Bae, S. Chen, A. Khademhosseini, Microfabrication of complex porous tissue engineering scaffolds using 3D projection stereolithography, *Biomaterials* 33 (2012) 3824–3834.
- [63] R. Lozano, L. Stevens, B.C. Thompson, K.J. Gilmore, R. Gorkin, E.M. Stewart, M. in het Panhuis, M. Romero-Ortega, G.G. Wallace, 3D printing of layered brain-like structures using peptide modified gellan gum substrates, *Biomaterials* 67 (2015) 264–273.
- [64] A. Isaacson, S. Swioklo, C.J. Connon, 3D bioprinting of a corneal stroma equivalent, *Exp. Eye Res.* 173 (2018) 188–193.
- [65] J.S. Lee, J.M. Hong, J.W. Jung, J.H. Shim, J.H. Oh, D.W. Cho, 3D printing of composite tissue with complex shape applied to ear regeneration, *Biofabrication* 6 (2014). 024103(1)–024103(12).
- [66] J. Suwanprateeb, R. Sanngam, W. Suvannapurk, T. Panyathanmaporn, Mechanical and in vitro performance of apatite—wollastonite glass ceramic reinforced hydroxyapatite composite fabricated by 3D-printing, *J. Mater. Sci Mater. Med.* 20 (2009) 1281–1289.
- [67] C. Bergmann, M. Lindner, W. Zhang, K. Koczur, A. Kirsten, R. Telle, H. Fischer, 3D printing of bone substitute implants using calcium phosphate and bioactive glasses, *J. Eur. Ceram. Soc.* 30 (2010) 2563–2567.
- [68] X. Wei, D. Li, W. Jiang, Z. Gu, X. Wang, Z. Zhang, Z. Sun, 3D Printable Graphene Composite, *Sci. Rep.* 5 (2015). 11181(1)–11181(7).
- [69] T. Xu, K.W. Binder, M.Z. Albanna, D. Dice, W. Zhao, J.J. Yoo, A. Atala, Hybrid printing of mechanically and biologically improved constructs for cartilage tissue engineering applications, *Biofabrication* 5 (2013). 015001(1)–015001(10).
- [70] F. Kotz, K. Arnold, W. Bauer, D. Schild, N. Keller, K. Sachsenheimer, T.M. Nargang, C. Richter, D. Helmer, B.E. Rapp, Three-dimensional printing of transparent fused silica glass, *Nature* 544 (2017) 337–339.
- [71] D.B. Kolesky, R.L. Truby, A.S. Gladman, T.A. Busbee, K.A. Homan, J.A. Lewis, 3D bioprinting of vascularized, heterogeneous cell-laden tissue constructs, *Adv. Mater.* 26 (2014) 3124–3130.
- [72] E.M. Gonçalves, F.J. Oliveira, R.F. Silva, M.A. Neto, M.H. Fernandes, M. Amaral, M. Vallet-Regí, M. Vila, Three-dimensional printed PCL-hydroxyapatite scaffolds filled with CNTs for bone cell growth stimulation, *J. Biomed. Mater. Res. B Appl. Biomater.* 104 (2016) 1210–1219.
- [73] K. Markstedt, A. Mantas, I. Tournier, H. Martínez Ávila, D. Hägg, P. Gatenholm, 3D bioprinting human chondrocytes with nanocellulose-alginate bioink for cartilage tissue engineering applications, *Biomacromolecules* 16 (2015) 1489–1496.

- [74] F.C. Fierz, F. Beckmann, M. Huser, S.H. Irsen, B. Leukers, A. Andronache, M. Thie, B. Mu, F. Witte, *Biomaterials* The morphology of anisotropic 3D-printed hydroxyapatite scaffolds, *Biomaterials* 29 (2008) 3799–3806.
- [75] R. Langer, J.P. Vacanti, *Tissue engineering*, *Science* 260 (1993) 920–926.
- [76] D. Howard, L.D. Buttery, K.M. Shakesheff, S.J. Roberts, *Tissue engineering: strategies, stem cells and scaffolds*, *J. Anat.* 213 (2008) 66–72.
- [77] S. Yang, K.F. Leong, Z. Du, C.K. Chua, *The design of scaffolds for use in tissue engineering. Part I. Traditional factors*, *Tissue Eng.* 7 (2001) 679–689.
- [78] S. MacNeil, *Progress and opportunities for tissue-engineered skin*, *Nature* 445 (2007) 874–880.
- [79] J. Hendriks, J. Riesle, C.A. van Blitterswijk, *Co-culture in cartilage tissue engineering*, *J. Tissue Eng. Regen. Med.* 1 (2010) 170–178.
- [80] C. Mandrycky, Z. Wang, K. Kim, D.H. Kim, *3D bioprinting for engineering complex tissues*, *Bio-technol. Adv.* 34 (2016) 422–434.
- [81] I. Zein, D.W. Huttmacher, K.C. Tan, S.H. Teoh, *Fused deposition modeling of novel scaffold architectures for tissue engineering applications*, *Biomaterials* 23 (2002) 1169–1185.
- [82] M.O. Wang, C.E. Vorwald, M.L. Dreher, E.J. Mott, M.-H. Cheng, A. Cinar, H. Mehdizadeh, S. Somo, D. Dean, E.M. Brey, J.P. Fisher, *Evaluating 3D-printed biomaterials as scaffolds for vascularized bone tissue engineering*, *Adv. Mater.* 27 (2015) 138–144.
- [83] R. Trombetta, J.A. Inzana, E.M. Schwarz, S.L. Kates, H.A. Awad, *3D printing of calcium phosphate ceramics for bone tissue engineering and drug delivery*, *Ann. Biomed. Eng.* 45 (2017) 23–44.
- [84] A.E. Jakus, A.L. Rutz, S.W. Jordan, A. Kannan, S.M. Mitchell, C. Yun, K.D. Koube, S.C. Yoo, H.E. Whiteley, C.-P. Richter, R.D. Galiano, W.K. Hsu, S.R. Stock, E.L. Hsu, R.N. Shah, *Hyperelastic “bone”: a highly versatile, growth factor—free, osteoregenerative, scalable, and surgically friendly biomaterial*, *Sci. Transl. Med.* 8 (2016). 358ra127(1)–358ra127(15).
- [85] A. Khalyfa, S. Vogt, J. Weisser, G. Grimm, A. Rechtenbach, W. Meyer, M. Schnabelrauch, *Development of a new calcium phosphate powder-binder system for the 3D printing of patient specific implants*, *J. Mater. Sci. Mater. Med.* 18 (2007) 909–916.
- [86] B. Duan, L.A. Hockaday, K.H. Kang, J.T. Butcher, *3D bioprinting of heterogeneous aortic valve conduits with alginate/gelatin hydrogels*, *J. Biomed. Mater. Res. A* (2013) 1255–1264.
- [87] J. Jang, H.J. Park, S.W. Kim, H. Kim, J.Y. Park, S.J. Na, H.J. Kim, M.N. Park, S.H. Choi, S.H. Park, S.W. Kim, S.M. Kwon, P.J. Kim, D.W. Cho, *3D printed complex tissue construct using stem cell-laden decellularized extracellular matrix bioinks for cardiac repair*, *Biomaterials* 112 (2017) 264–274.
- [88] A. Faulkner-Jones, C. Fyfe, D.-J. Cornelissen, J. Gardner, J. King, A. Courtney, W. Shu, *Bioprinting of human pluripotent stem cells and their directed differentiation into hepatocyte-like cells for the generation of mini-livers in 3D*, *Biofabrication* 7 (2015) 044102.
- [89] H. Lee, D.-W. Cho, *One-step fabrication of an organ-on-a-chip with spatial heterogeneity using a 3D bioprinting technology*, *Lab Chip* 16 (2016) 2618–2625.
- [90] J. Banks, *Adding value in additive manufacturing: researchers in the United Kingdom and Europe look to 3D printing for customization*, *IEEE Pulse.* 4 (2013) 22–26.
- [91] L.E. Diment, M.S. Thompson, J.H.M. Bergmann, *Clinical efficacy and effectiveness of 3D printing: a systematic review*, *BMJ Open.* 7 (2017). e016891(1)–e016891(11).
- [92] J. Parthasarathy, *3D modeling, custom implants and its future perspectives in craniofacial surgery*, *Ann. Maxillofac. Surg.* 4 (2014) 9–18.
- [93] F. Rengier, A. Mehndiratta, H. Von Tengg-Kobligk, C.M. Zechmann, R. Unterhinninghofen, H.U. Kauczor, F.L. Giesel, *3D printing based on imaging data: review of medical applications*, *Int. J. Comput. Assist. Radiol. Surg.* 5 (2010) 335–341.
- [94] A.J. Reiffel, C. Kafka, K.A. Hernandez, S. Popa, J.L. Perez, S. Zhou, S. Pramanik, B.N. Brown, W.S. Ryu, L.J. Bonassar, J.A. Spector, *High-fidelity tissue engineering of patient-specific auricles for reconstruction of pediatric microtia and other auricular deformities*, *PLoS One.* 8 (2013) e56506(1)–e56506(8).
- [95] C.H. Lee, J.L. Cook, A. Mendelson, E.K. Moioli, H. Yao, J.J. Mao, *Regeneration of the articular surface of the rabbit synovial joint by cell homing: a proof of concept study*, *Lancet* 376 (2010) 440–448.

- [96] C.H. Lee, S.A. Rodeo, L.A. Fortier, C. Lu, C. Erisken, J.J. Mao, Protein-releasing polymeric scaffolds induce fibrochondrocytic differentiation of endogenous cells for knee meniscus regeneration in sheep, *Sci Ence Transl. Med.* 6 (2014). 266ra171(1)–266ra171(21).
- [97] R.J. Morrison, S.J. Hollister, M.F. Niedner, M.G. Mahani, A.H. Park, D.K. Mehta, R.G. Ohye, G.E. Green, Mitigation of tracheobronchomalacia with 3D-printed personalized medical devices in pediatric patients, *Sci. Transl. Med.* 7 (2015). 285ra64(1)–285ra64(23).
- [98] S. Bose, S. Vahabzadeh, A. Bandyopadhyay, Bone tissue engineering using 3D printing, *Mater. Today* 16 (2013) 496–504.
- [99] F.A. Probst, D.W. Huttmacher, D.F. Müller, H.–G. Machens, J.–T. Schantz, Rekonstruktion der Kalvaria durch ein präfabriziertes bioaktives Implantat TT—calvarial reconstruction by customized bioactive implant, *Handchir. Mikrochir. Plast. Chir.* 42 (2010) 369–373.
- [100] A. Cohen, A. Laviv, P. Berman, R. Nashef, J. Abu-Tair, Mandibular reconstruction using stereolithographic 3-dimensional printing modeling technology, *Oral Surg. Oral Med. Oral Pathol. Oral Radiol. Endodontol.* 108 (2009) 661–666.
- [101] I. Wolf, M. Vetter, I. Wegner, T. Böttger, M. Nolden, M. Schöbinger, M. Hastenteufel, T. Kunert, H.–P. Meinzer, The medical imaging interaction toolkit, *Med. Image Anal.* 9 (2005) 594–604.
- [102] D. Mitsouras, P. Liacouras, A. Imanzadeh, A.A. Giannopoulos, T. Cai, K.K. Kumamaru, E. George, N. Wake, E.J. Caterson, B. Pomahac, V.B. Ho, G.T. Grant, F.J. Rybicki, Medical 3D printing for the radiologist, *RadioGraphics* 35 (2015) 1965–1988.
- [103] R. Sharma, Forbes, <https://www.forbes.com/sites/rakeshsharma/2013/07/08/the-3d-printing-revolution-you-have-not-heard-about/#6e6aa35c1a6b>, 2018. Accessed 4 July 2018.
- [104] EnvisionTEC, <https://envisiontec.com/3d-printing-materials>, 2018. Accessed 25 July 2018.
- [105] So Sonova, <https://www.sonova.com/en/features/3d-printing-technology-improved-hearing>, 2018. Accessed 3 August 2018.
- [106] A.H. Jassim-Jaboori, M.O. Oyewumi, 3D printing technology in pharmaceutical drug delivery: prospects and challenges, *J. Biomol. Res. Ther.* 04 (2015). 1000e141(1)–1000e141(3).
- [107] S.A. Khaled, J.C. Burley, M.R. Alexander, C.J. Roberts, Desktop 3D printing of controlled release pharmaceutical bilayer tablets, *Int. J. Pharm.* 461 (2014) 105–111.
- [108] W. Huang, Q. Zheng, W. Sun, H. Xu, X. Yang, Levofloxacin implants with predefined microstructure fabricated by three-dimensional printing technique, *Int. J. Pharm.* 339 (2007) 33–38.
- [109] Y. Gu, X. Chen, J.–H. Lee, D.A. Monteiro, H. Wang, W.Y. Lee, Inkjet printed antibiotic- and calcium-eluting bioresorbable nanocomposite micropatterns for orthopedic implants, *Acta Biomater.* 8 (2012) 424–431.
- [110] J. Pardeike, D.M. Strohmeier, N. Schrodll, C. Voura, M. Gruber, J.G. Khinast, A. Zimmer, Nanosuspensions as advanced printing ink for accurate dosing of poorly soluble drugs in personalized medicines, *Int. J. Pharm.* 420 (2011) 93–100.
- [111] A. Dawood, B.M. Marti, V. Sauret-Jackson, A. Darwood, 3D printing in dentistry, *Br. Dent. J.* 219 (2015) 521–529.
- [112] A. Hazeveld, J.J.R. Huddleston Slater, Y. Ren, Accuracy and reproducibility of dental replica models reconstructed by different rapid prototyping techniques, *Am. J. Orthod. Dentofac. Orthop.* 145 (2014) 108–115.
- [113] T. McCue, Forbes, <https://www.forbes.com/sites/tjmccue/2017/09/14/3d-printing-moves-align-technology-toward-1-3-billion-in-sales/#4b02b8b45378>, 2018. Accessed 1 September 2018.
- [114] Invisalign, <https://www.invisalign.co.uk/en/what-is-invisalign/Pages/Technology.aspx>, 2018. Accessed 16 August 2018.
- [115] C. Li, Y. Chen, Multilayer Dental Appliances and Related Methods and Systems, 2012. US20130302742A1.
- [116] R.L. Boyd, R.J. Miller, The invisalign system in adult orthodontics: mild crowding and space closure cases, *J. Clin. Orthod.* XXXIV (2000) 203–212.
- [117] G. Rasperini, S.P. Pilipchuk, C.L. Flanagan, C.H. Park, G. Pagni, S.J. Hollister, W.V. Giannobile, 3D-printed bioresorbable scaffold for periodontal repair, *J. Dent. Res.* 94 (2015) 153S–157S.
- [118] F. Momeni, S.M. Mehdi Hassani, X. Liu, J. Ni, A review of 4D printing, *Mater. Des.* 122 (2017) 42–79.
- [119] S. Ramesh, S. Kiran reddy, C. Usha, N.K. Naulakha, C. Adithyakumar, M. Lohith Kumar Reddy, Advancements in the research of 4D printing—a review, *IOP Conf. Ser. Mater. Sci. Eng.* 376 (2018) 012123.

- [120] Z.X. Khoo, J.E.M. Teoh, Y. Liu, C.K. Chua, S. Yang, J. An, K.F. Leong, W.Y. Yeong, 3D printing of smart materials: a review on recent progresses in 4D printing, *Virtual Phys. Prototyp.* 10 (2015) 103–122.
- [121] M. Nadgorny, Z. Xiao, C. Chen, L.A. Connal, Three-dimensional printing of pH-responsive and functional polymers on an affordable desktop printer, *ACS Appl. Mater. Interfaces* 8 (2016) 28946–28954.
- [122] A.T. Clare, P.R. Chalker, S. Davies, C.J. Sutcliffe, S. Tsopanos, Selective laser melting of high aspect ratio 3D nickel-titanium structures two way trained for MEMS applications, *Int. J. Mech. Mater. Des.* 4 (2008) 181–187.
- [123] M. López-Valdeolivas, D. Liu, D.J. Broer, C. Sánchez-Somolinos, 4D printed actuators with soft-robotic functions, *Macromol. Rapid Commun.* 39 (2018) 3–9.
- [124] S.A. Khaled, J.C. Burley, M.R. Alexander, J. Yang, C.J. Roberts, 3D printing of five-in-one dose combination polypill with defined immediate and sustained release profiles, *J. Control. Release* 217 (2015) 308–314.
- [125] M. Rocca, A. Fragasso, W. Liu, M.A. Heinrich, Y.S. Zhang, Embedded multimaterial extrusion bioprinting, *SLAS Technol.* 23 (2018) 154–163.
- [126] A. Inamdar, M. Magana, F. Medina, Y. Grajeda, R. Wicker, Development of an automated multiple material stereolithography machine, in: *Proc. 17th Annu. Solid Free. Fabr. Symp.*, 2006, pp. 624–635.
- [127] D. Chen, X. Zheng, Multi-material additive manufacturing of metamaterials with giant, tailorable negative poisson's ratios, *Sci. Rep.* 8 (2018). 9139(1)–9139(8).
- [128] T. Laumer, M. Karg, M. Schmidt, Laser beam melting of multi-material components, *Phys. Procedia* 39 (2012) 518–525.
- [129] Y. Chivel, New approach to multi-material processing in selective laser melting, *Phys. Procedia* 83 (2016) 891–898.
- [130] A.J. Lopes, E. MacDonald, R.B. Wicker, Integrating stereolithography and direct print technologies for 3D structural electronics fabrication, *Rapid Prototyp. J.* 18 (2012) 129–143.
- [131] S. Wang, J.M. Lee, W.Y. Yeong, Smart hydrogels for 3D bioprinting, *Int. J. Bioprint.* 1 (2015) 1–14.
- [132] S. Dutta, D. Cohn, Temperature and pH responsive 3D printed scaffolds, *J. Mater. Chem. B* 5 (2017) 9514–9521.
- [133] D. Han, C. Farino, C. Yang, T. Scott, D. Browe, W. Choi, J.W. Freeman, H. Lee, Soft robotic manipulation and locomotion with a 3D printed electroactive hydrogel, *ACS Appl. Mater. Interfaces* 10 (2018) 17512–17518.
- [134] A.S. Gladman, E.A. Matsumoto, R.G. Nuzzo, L. Mahadevan, J.A. Lewis, Biomimetic 4D printing, *Nat. Mater.* 15 (2016) 413–418.
- [135] Z. Xiong, C. Zheng, F. Jin, R. Wei, Y. Zhao, X. Gao, Y. Xia, X. Dong, M. Zheng, X. Duan, Magnetic-field-driven ultra-small 3D hydrogel microstructures: preparation of gel photoresist and two-photon polymerization microfabrication, *Sens. Actuators B Chem.* 274 (2018) 541–550.
- [136] A. Lendlein, R. Langer, Biodegradable, elastic shape-memory polymers for potential biomedical applications, *Science* 296 (2002) 1673–1676.
- [137] F. El Feninat, G. Laroche, M. Fiset, D. Mantovani, Shape memory materials for biomedical applications, *Av. Eng. Mater.* 4 (2002) 91–104.
- [138] K. Kratz, U. Voigt, A. Lendlein, Temperature-memory effect of copolyesterurethanes and their application potential in minimally invasive medical technologies, *Adv. Funct. Mater.* 22 (2012) 3057–3065.
- [139] C.M. Yakacki, R. Shandas, C. Lanning, B. Rech, A. Eckstein, K. Gall, Unconstrained recovery characterization of shape-memory polymer networks for cardiovascular applications, *Biomaterials* 28 (2007) 2255–2263.
- [140] A. Lendlein, S. Kelch, Shape-memory effect from permanent shape, *Angew. Chem.* 41 (2002) 2034–2057.
- [141] M. Zarek, N. Mansour, S. Shapira, D. Cohn, 4D printing of shape memory-based personalized endoluminal medical devices, *Macromol. Rapid Commun.* 38 (2017) 1600628.
- [142] Q. Ge, A.H. Sakhaei, H. Lee, C.K. Dunn, N.X. Fang, M.L. Dunn, Multimaterial 4D printing with tailorable shape memory polymers, *Sci. Rep.* 6 (2016). 31110(1)–31110(11).
- [143] C.L. Ventola, Medical applications for 3D printing: current and projected uses, *P T.* 39 (2014) 704–711.

- [144] D. Garcia-Gonzalez, S. Garzon-Hernandez, A. Arias, A new constitutive model for polymeric matrices: application to biomedical materials, *Compos. B Eng.* 139 (2018) 117–129.
- [145] D.C. Ackland, D. Robinson, M. Redhead, P.V.S. Lee, A. Moskaljuk, G. Dimitroulis, A personalized 3D-printed prosthetic joint replacement for the human temporomandibular joint: from implant design to implantation, *J. Mech. Behav. Biomed. Mater.* 69 (2017) 404–411.
- [146] R.K. Chen, Y. Jin, J. Wensman, A. Shih, Additive manufacturing of custom orthoses and prostheses—a review, *Addit. Manuf.* 12 (2016) 77–89.
- [147] J. Norman, R.D. Madurawe, C.M.V. Moore, M.A. Khan, A. Khairuzzaman, A new chapter in pharmaceutical manufacturing: 3D-printed drug products, *Adv. Drug Deliv. Rev.* 108 (2017) 39–50.
- [148] A.L. Jardini, M.A. Larosa, R.M. Filho, C.A.D.C. Zavaglia, L.F. Bernardes, C.S. Lambert, D. R. Calderoni, P. Kharmandayan, Cranial reconstruction: 3D biomodel and custom-built implant created using additive manufacturing, *J. Cranio-Maxillofac. Surg.* 42 (2014) 1877–1884.